Development of Catalytic Strategies and Microreactor Technology for the Synthesis of Bio-based Furanics from Lignocellulosederived Carbohydrates

Guo, Wenze

DOI:
10.33612/diss.178033475

CHAPTER 4

Continuous Synthesis of 5-Hydroxymethyl-furfural from Glucose Using a Combination of $AlCl_3$ and HCl as Catalyst in a Biphasic Slug Flow Capillary Microreactor

This chapter is published as:

Guo, W.; Heeres, H. J.; Yue, J., Continuous synthesis of 5-hydroxymethylfurfural from glucose using a combination of $AlCl_3$ and HCl as catalyst in a biphasic slug flow capillary microreactor. *Chemical Engineering Journal*. 2020, 381, 122754. DOI: 10.1016/j.cej.2019.122754.

Abstract

5-Hydroxymethylfurfural (HMF) was synthesized from glucose in a slug flow capillary microreactor, using a combination of $AlCl_3$ and HCl as the homogeneous catalyst in the aqueous phase and methyl isobutyl ketone as the organic phase for in-situ HMF extraction. After optimization, an HMF yield of 53% was obtained at a pH of 1.5, 160 ^oC and a residence time of 16 min, and it could be further increased to 66.2% by adding 20 wt% NaCl in the aqueous phase. Slug flow operation in the microreactor greatly promoted mixing/reaction in the aqueous droplet and facilitated HMF extraction to the organic slug, enabling the reaction to run (largely) under kinetic control and an enhanced HMF yield by suppressing its further rehydration, degradation and/or polymerization. Confining reaction in the aqueous droplet prevented humin deposition on the microreactor wall. In line with the literature, $[Al(OH)_2]^+$ was confirmed by ESI-MS as the catalytically active species, and is responsible for the glucose isomerization to fructose under various pH values. The ratio between $AlCl_3$ and HCl was optimized for the highest HMF yield and the best results were obtained with 40 mM $AlCl_3$ and 40 mM HCl. Compared with batch results, a higher HMF yield was obtained in the microreactor at the same reaction time mainly due to a higher heating rate therein. The aqueous catalyst was recycled and reused three times without a noticeable performance loss. Thus, the present recyclable and stable homogenous catalyst system, combined with biphasic microreactor operation, is an attractive concept for the glucose conversion to HMF.

4.1. Introduction

Diminishing fossil resources and growing environmental concerns over greenhouse gas emissions have spurred research efforts towards utilizing biomass for the production of fuels, chemicals and performance materials. High attention is currently given to the conversion of lignocellulosic biomass (the most abundant biomass in nature) to 5-hydroxymethylfurfural (HMF). HMF is a versatile platform chemical which can be converted into derivatives with applications as biofuels, biobased polymers and chemicals[1-3]. For example, the selective oxidation of HMF yields 2,5-furandicarboxylic acid[4], a building block to make polyethylene furanoate (PEF), which is a promising replacement for petroleum-based polyethylene terephthalate (PET)[5]. The selective hydrogenation of HMF yields 2,5-dimethylfuran and 2-methylfuran[6], which have potential as liquid transportation fuel additives[7]. HMF can also be

rehydrated to levulinic acid[8], an interesting platform chemical which for instance can be hydrogenated to γ-valerolactone[9,10].

HMF is typically produced by the dehydration of lignocellulosic hexoses such as fructose and glucose. HMF yields are a strong function of the hexose used, with fructose giving by far better results than glucose[11,12] . However, glucose is a more attractive source for HMF synthesis as it is cheaper than pure fructose and fructose rich sources (inulin, high fructose corn syrup)[13-15]. To be able to use glucose as the feed, the in-situ isomerization of glucose to fructose followed by the subsequent dehydration to HMF has gained high research attention [11,16-19]. High HMF yields from glucose are attainable in ionic liquids[20,21] and aprotic organic solvents[22,23] using various mineral salts as Lewis acid catalysts. However, the usually high price of ionic liquids and the difficult downstream separation of HMF from the high-boiling solvents are still issues to be solved. Consequently, water as a green and cheap solvent is preferred as the reaction medium for large scale HMF production. However, in water the yield of HMF from glucose is limited due to various parallel and series reactions to among others levulinic acid, formic acid, soluble and insoluble oligomers/polymers (collectively known as humins)[24]. To increase yields, biphasic systems (consisting of an aqueous phase for the reaction and an organic phase for in-situ HMF extraction) have been developed and experimentally proven to be effective for improving HMF yield[25,26]. Usually heterogeneous catalysts are preferred over homogeneous ones due to the ease of catalyst separation and reuse[19,27,28]. However, humins may deposit on the catalyst and block active sites and pores, requiring advanced catalyst regeneration procedures.

In the past years, several homogeneous Lewis acid catalysts such as Cr(III), Al(III), Zn(II) and Sn(IV) have been reported to be active for the isomerization of glucose to fructose in the aqueous solution and this opens the opportunity for a concept where glucose is in-situ isomerized to fructose, which is subsequently converted to HMF in high yields[11,15,16,24,29-31]. However, Cr(III) and Sn(IV) are toxic and carcinogenic. As for Zn(II), a rather high concentration is required to catalyze the glucose conversion, and it is soluble in methyl isobutyl ketone (MIBK), a common organic solvent for HMF extraction, causing HMF-involved side reactions and catalyst loss[29]. In contrast, Al(III) (e.g., in the form of $AlCl_3$) is cheap and has a low toxicity. HMF yields over 40% from glucose have been reported using $AlCl_3$ (and HCl) as catalyst in biphasic systems in batch reactors[11,15,18,24,30]. However, improvements are required such as i)

identification of extraction solvents with high HMF partition which are less expensive and toxic than those like alkylphenolics; ii) improved space time yields as reactions were typically investigated in laboratory batch reactors with low substrate concentrations and long reaction times (e.g., ca. 1 h or more); iii) development of efficient catalyst recycle strategies. In addition, relatively little is known about the active species when using $AlCl_3$ as the catalyst. It is known to hydrolyze rapidly in water to form various species (e.g., $[Al(H_2O)_6]^{3+}$, $[Al(OH)(H_2O)_5]^{2+}$ and $[Al(OH)_2(H_2O)_4]^{+}$) depending on the pH value, $AlCl_3$ concentration and temperature[32]. Therefore, identification of the active Al species and their role in regulating the glucose conversion network is of high interest.

Compared with conventional batch reactors (especially on a large scale), continuous flow processing in microreactors has certain advantages such as much higher heat and mass transfer rates leading to higher space time yields[33-37]. In the past years, the use of microreactors for the synthesis of HMF or 5-chloromethylfurfural (CMF) from fructose in single phase or biphasic systems has been investigated[38-44]. For instance, Shimanouchi et al. [40,41] developed a simplified kinetic model for slug flow operation and suggested that the vortex field generated in slug flow likely contributed to an increase in HMF mass transfer rates. However, there have been fewer reports about the application of microreactors for the conversion of glucose to HMF. Recently, Muranaka et al.[39] demonstrated HMF synthesis from sugars in a slug flow capillary microreactor (made of stainless steel) using 2-*sec*-butyl phenol as the extraction solvent and a phosphate saline buffer as catalyst. HMF yields of 80.9% and 75.7% could be obtained from fructose and glucose, respectively, at 180 ^{o}C after 47 min residence time. Despite the high HMF yield (primarily due to the high HMF partition into 2-sec-butyl phenol), the solvent is expensive and toxic, catalyst recyclability was not examined, and relatively long residence times negatively affect the space time yield. Besides, solid humins as a byproduct could accumulate and adhere to the inner wall of the stainless steel microreactor since the aqueous reaction phase was the continuous phase, potentially causing reactor blockage (an important issue to be mitigated for flow processing in microreactors).

We here report for the first time a systematic experimental study on HMF synthesis from glucose in a biphasic system in a slug flow capillary microreactor, using a combination of $AlCl_3$ and HCl as the homogeneous catalyst and MIBK as the extraction solvent (cheap, low toxicity, acceptable HMF partition capacity compared to its counterparts). A perfluoroalkoxy alkane

(PFA) capillary microreactor was used to ensure that the aqueous reaction phase is present as droplets and thus not in direct contact with the microreactor wall to avoid humin deposition on the reactor wall causing reactor blockage. The roles of $AlCl_3$ and HCl in the reaction network of the glucose conversion were investigated by performing experiments with glucose, fructose and HMF as the substrate. The reaction conditions were screened, with a focus on the ratio between $AlCl_3$ and HCl which was investigated to regulate the reaction network and thus to optimize the HMF yield. Advanced mass spectroscopy on model reactants and product samples was performed to investigate the variation of the catalytic active Al species present in solution with Brønsted acidity, and to explain the pH dependency of the glucose conversion and the possible intermediates in the reaction network. Moreover, a performance comparison with a laboratory batch reactor as well as the literature work was made to highlight the potential of microreactors, and the recyclability and reusability of the homogenous catalyst system were demonstrated.

4.2. Experimental section

4.2.1. Materials

D-glucose (99 wt%), D-fructose (99 wt%), D-mannose (99 wt%), methyl isobutyl ketone (MIBK, 99 wt%) were purchased from Acros Organics Co., Ltd. Aluminum chloride hexahydrate (99 wt%), hydrochloric acid (37 wt%), 5-hydroxymethylfurfural (99 wt%), formic acid (99 wt%), levulinic acid (99 wt%) and lactic acid (99.0 wt%) were all purchased from Sigma-Aldrich Co., Ltd. All chemicals were of chemical grade and used as received without any further treatment. PFA tubings (inner diameter: 1.65 mm) were used as capillary microreactors and supplied by Swagelok company.

4.2.2. Experimental setup and procedure

Fig. 4.1 shows the experimental setup for HMF synthesis in the slug flow capillary microreactor, which was designed and built based on the previously reported work for HMF or CMF synthesis in microreactors[38-43]. Typically, the aqueous feed consisted of glucose and the $AlCl_3$/HCl catalyst, and the organic feed consisted of MIBK. Both phases were fed to the microreactor using a binary HPLC pump unit (Agilent 1200 Series) at an organic to aqueous volumetric flow ratio of 4 to 1. The two phases were mixed in a polyether ether ketone (PEEK)

Y-connector (inner diameter: 1.65 mm) to generate a uniform slug flow in the downstream PFA capillary microreactor. The microreactor was coiled around an aluminum block and placed in an oven at 160 °C. The microreactor exit was passed through a water bath (ca. 20 °C) to quench the reaction. A back pressure regulator was installed at the end of the microreactor to maintain a constant pressure of around 10 bar in the microreactor to keep the reactor content in the liquid state. Product samples were collected after the system reached steady state (i.e., after approximately 4 times the residence time in the microreactor). The length of the microreactor (i.e., excluding very short sections outside the oven which were kept at room temperature and thus without appreciable reaction occurrence) is typically 4.5 m. For experiments aimed at investigating the role of mass transfer on performance, microreactors of 1.2 m and 17 m length were also used. The residence time (τ) in the microreactor was varied by adjusting the flow rates (details about the calculation of τ and the actual flow rates are given in Tables S4.1 and S4.2 in the Supplementary material).

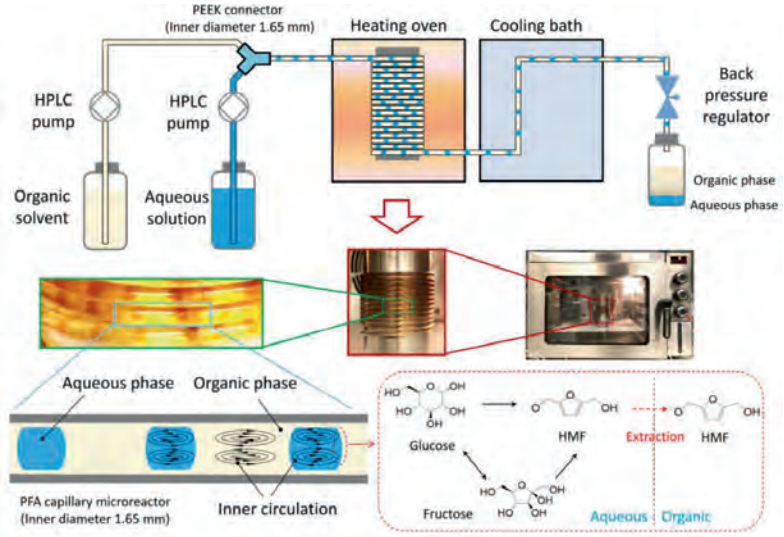

Fig. 4.1. Schematic diagram of the slug flow capillary microreactor system for continuous HMF synthesis from glucose. The inner circulation in droplets and slugs promoted mixing/reaction in the aqueous phase and enhanced in-situ extraction of HMF to the organic phase.

The collected aqueous and organic phases were filtered through a polytetrafluoroethylene

(PTFE, 0.45 μm) filter, and subsequently analyzed by high performance liquid chromatography (HPLC) and gas chromatography (GC), respectively. To elucidate the role of $AlCl_3$ and HCl in the glucose conversion reaction network, the aqueous phases containing different substrates (glucose, fructose, HMF) and catalysts (HCl or $AlCl_3$ only) were also tested in the same setup.

Some additional experiments in the microreactor have been performed to study the influence of the reaction temperature, the organic to aqueous volumetric flow ratio, the extraction solvent type (i.e., using methyltetrahydrofuran) and the addition of salt (i.e., NaCl) in the aqueous phase on the reaction performance with the purpose of further optimizing the HMF yield. The other experimental details remained unchanged as shown above.

4.2.3. Analyses and characterization

The composition of the aqueous phase was analyzed by an Agilent 1200 HPLC, equipped with an Agilent 1200 pump, a refractive index detector, a standard ultraviolet detector as well as a Bio-Rad organic acid column (Aminex HPX-87H). A diluted aqueous H_2SO_4 solution (5 mM, 0.55 mL/min) was used as the eluent, and the temperature of the column was maintained at 60 °C. The analysis was complete within 60 min. The organic phase was analyzed by a TraceGC ultra GC, equipped with a flame ionization detector and a fused silica column (Stabilwax-DA). The concentrations of the components in the aqueous and organic samples were determined from the calibration curves obtained using the standard solutions with known concentrations.

GC–MS analysis was performed to further identify the components (e.g. HMF, levulinic acid, furfural) in the organic product samples, using an HP6890 GC equipped with an HP1 column (dimethylpolysiloxane; length of 25 m; inside diameter of 0.25 mm; film thickness of 0.25 μm) in combination with an HP5973 mass selective detector. Peaks were identified using the NIST05a mass spectral library.

Inducted coupled plasma atomic emission spectroscopy analyses (ICP-AES) were performed using an Optima 7000 DV Optical Emission Spectrometer (PerkinElmer, USA) to quantify the amount of Al species in the organic phase.

Dynamic light scattering (DLS) was performed on a Brookhaven ZetaPALS instrument to determine the presence of solid particles after the reaction. Fresh aqueous solutions of $AlCl_3$ (40 mM), $AlCl_3$/HCl (40 mM/40 mM) were prepared and analyzed. In addition, samples after a thermal treatment were investigated. For this purpose, the fresh solutions were filtered

using a syringe filter (0.45 μm; PTFE), and heated at 160 ℃ for 20 min. It was assumed that the viscosity of the solutions was equal to that of water. The data were analyzed using the Multimodal Size Distribution algorithm of the software.

Electro-spray ionization mass spectra (ESI-MS) were recorded on an Orbitrap XL mass spectrometer (Thermo Fisher Scientific) with ESI ionization in the positive mode. Samples including the fresh and recycled glucose solutions containing $AlCl_3$ and HCl were measured in the range of *m*/*z* 100-600 with the following operating parameters: capillary voltage at 3.2 kV, sample cone voltage at 40 V, vaporizer temperature of the source at 150 °C, cone gas (N_2) flow at 20 L/h, injection volume of 5 μL. A collision energy of 20 eV was used for the collision-induced dissociation stage in the MS/MS measurements. The data acquisition and analyses were performed using Xcalibur software.

4.2.4. Definitions and calculations

The conversion of substrate i (X_i) and the yield of product j (Y_j) in the microreactor are defined by Eqs. 4.1 and 4.2.

$$X_i = \frac{Q_{aq,0}C_{aq,i,0} - Q_{aq,1}C_{aq,i,1}}{Q_{aq,0}C_{aq,i,0}} \times 100\% \tag{4.1}$$

$$Y_j = \frac{Q_{org,1}C_{org,j,1} + Q_{aq,1}C_{aq,j,1}}{Q_{aq,0}C_{aq,i,0}} \times 100\% \tag{4.2}$$

In the above equations, $Q_{aq,0}$ and $Q_{org,0}$ refer to the flow rates of the aqueous and organic phases at the microreactor inlet (at ca 20 °C), respectively. $Q_{aq,1}$ and $Q_{org,1}$ refer to the flow rates of the aqueous and organic phases at the microreactor outlet (at ca. 20 °C), respectively. $C_{aq,i,0}$ and $C_{aq,i,1}$ are the concentrations of substrate i in the aqueous solutions at the microreactor inlet and outlet, respectively. $C_{aq,j,1}$ and $C_{org,j,1}$ represent the concentrations of product j in the aqueous and organic phases at the microreactor outlet, respectively. Due to the partial miscibility of MIBK and water, the volumetric flow rates of the two phases at the microreactor outlet ($Q_{aq,1}$ and $Q_{org,1}$) differ from the inlet flow rates, and were corrected as

$$Q_{aq,1} = Q_{aq,0}\alpha_{aq} \tag{4.3}$$

$$Q_{org,1} = Q_{org,0}\alpha_{org} \tag{4.4}$$

where α_{aq} or α_{org} is the correction factor which represents the ratio of the volumetric flow

rates at the microreactor outlet and inlet for either the aqueous or organic phase (see Table S4.3 in the Supplementary material for calculation details).

The carbon balance is defined in Eq. 4.5.

$$\text{C balance} = \frac{\text{C amount in the products} + \text{C amount in the remaining substrate}}{\text{C amount in the starting substrate}} \times 100\% \quad (4.5)$$

The carbon balance is based on the quantified products by HPLC and GC (including glucose, fructose, mannose, HMF, levulinic acid and formic acid). It does not account for the non-identified soluble/insoluble byproducts.

4.3. Results and discussion

4.3.1. HMF synthesis from glucose using a combined $AlCl_3$/HCl catalyst in a biphasic slug flow capillary microreactor

Experiments with glucose (0.1 M) in the microreactor were performed using a combination of $AlCl_3$ and HCl as catalyst at 160 ^oC in a water-MIBK biphasic system. A HMF yield of 53% was obtained at a glucose conversion of 95.8% and a residence time of 16 min using 40 mM $AlCl_3$ and 40 mM HCl (pH = 1.5 measured at 20 ^oC; Fig. 4.2). It is worth noting that here the reaction was conducted under the optimized temperature, $AlCl_3$/HCl ratio and MIBK to water volumetric flow ratio, and HMF yields can be further improved by enhancing the HMF partition into the organic phase, which will be discussed in detail hereafter. Good reproducibility was observed as is evident from the error bars provided in Fig. 4.2. Fructose was the primary product, together with small amounts of the epimerization product mannose. The yields of fructose, mannose and HMF showed clear maxima, indicating that these are intermediate products and prone to further chemistry[17]. The expected byproducts at longer residence times were LA and FA. In addition, HPLC and GC showed the presence of acetic acid and furfural, though in amounts less than 1%. The carbon balance closure was high at short residence times, though decreased rapidly, likely due to the formation of the unidentified soluble byproducts (by HPLC and GC) and higher molecular weight compounds such as humins (under these optimized reaction conditions little insoluble black solid humins were observed visually).

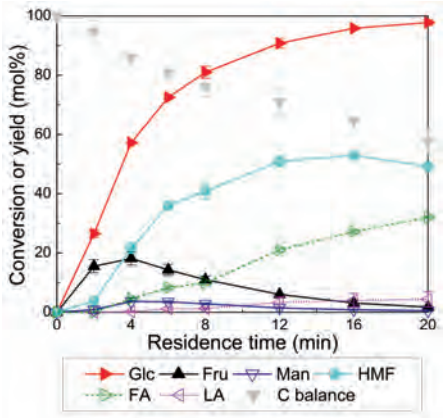

Fig. 4.2. HMF synthesis from glucose in a biphasic system in the slug flow capillary microreactor. Reaction conditions: 0.1 M glucose, microreactor length of 4.5 m, 160 °C, 40 mM $AlCl_3$ and 40 mM HCl (pH = 1.5 measured at 20 °C), 4:1 organic to aqueous flow ratio at the microreactor inlet (unless otherwise specified, the organic phase refers to MIBK). In the figure legend, Glu, Fru, Man, FA and LA denote glucose, fructose, mannose, formic acid and levulinic acid, respectively (the same in other figures shown hereafter).

Based on the literature data[16,24,30,45] and the current set of experiments, a typical glucose conversion network is provided in Fig. 4.3. The initial step involves the isomerization of glucose to a mixture of fructose, mannose and remaining glucose. This isomerization reaction is known to be equilibrium limited[46,47]. HMF is expected to be formed mainly via fructose dehydration and not from glucose dehydration. The latter reaction is known to be by far slower than the reaction from fructose[48], and as such of less importance than the reaction from fructose to HMF. HMF was not inert under the prevailing conditions and could be further rehydrated to produce equimolar FA and LA[45]. A stoichiometric excess of FA over LA was observed, suggesting that FA was also formed by other reaction pathways. A possibility is the formation directly from the degradation of sugars and HMF (leading to the formation of other byproducts like humins as well)[24,49]. Another possibility is the decomposition of HMF into furfural and formaldehyde[24,50,51], the latter is converted to FA, for instance by oxidation with the remaining air[24]. The possibility of LA conversion to among others levulinates or poly-condensated products[52] was excluded on the basis of control experiments using LA as the starting substrate at the same operational conditions (160 °C, 40 mM $AlCl_3$ and 40 mM HCl,

4:1 organic to aqueous inlet flow ratio) in the microreactor. Here, the LA conversion remained below 1% for a residence time of 20 min (Fig. S4.3 in the Supplementary material).

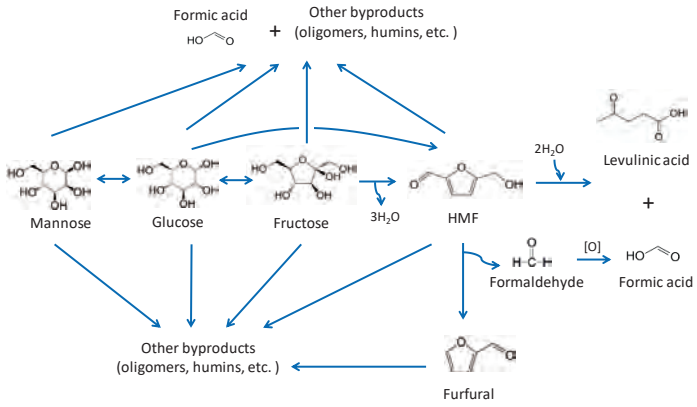

Fig. 4.3. Proposed reaction network for the glucose conversion to HMF.

It is known that at higher temperatures the $AlCl_3$ hydrolysis equilibrium tends to shift to the formation of $Al(OH)_3$ which subsequently precipitates irreversibly and thus would result in a pH decrease of the solution after the reaction[32], as was also found in the case of $CrCl_3$[17]. However, in our experiments shown in Fig. 4.2, pH of the solution was found nearly constant after the reaction. DLS measurements indicated the absence of the suspended particles in the heat-treated (160 °C, 20 min) aqueous solution of 40 mM $AlCl_3$ and 40 mM HCl, and thus no appreciable Al^{3+} loss in the form of $Al(OH)_3$ is expected.

Additionally, due to the presence of HCl in the reaction mixture, the hydroxyl group of HMF might be substituted by chlorine to form CMF in the aqueous phase followed by transfer of CMF to the organic phase. This reaction is well established for the dehydration of carbohydrates (e.g., fructose, glucose and sucrose) using highly concentrated HCl solutions (32 wt%; ca. 8.7 M) in biphasic continuous reactors[38,43]. However, CMF was not detected by GC-MS in the MIBK phase after the reaction for all experimental runs in this work, probably due to a much lower HCl concentration used by us (<< 1 M).

4.3.2. Role of catalyst components: experiments with glucose and reaction intermediates using $AlCl_3$ or HCl as catalyst in the slug flow capillary microreactor

Since $AlCl_3$ hydrolyzes in water to form Al species and HCl[32], the catalytic effects in the glucose conversion may be related to both of them. Thus, to better understand the roles of Lewis acid (Al species from $AlCl_3$) and Brønsted acid (HCl) in the glucose conversion network (Fig. 4.3) and to help optimize the microreactor performance, experiments with the individual catalyst components in combination with glucose, fructose or HMF were conducted in a water-MIBK biphasic system in the capillary microreactor in the slug flow regime. The reaction was catalyzed using either $AlCl_3$ (40 mM) or HCl (0.39 mM). In both cases the pH of the aqueous phase was 3.4 (measured at 20 °C).

4.3.2.1. Experiments with HMF

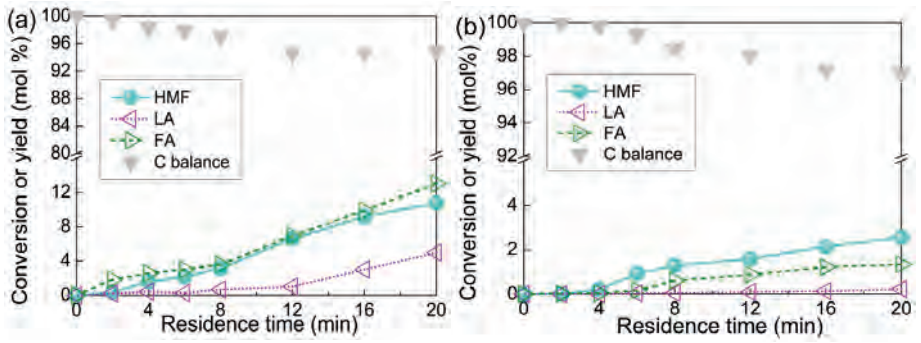

Fig. 4.4. Results of experiments with HMF as the substrate in a biphasic system in the slug flow capillary microreactor with (a) $AlCl_3$ and (b) HCl as catalyst. Other reaction conditions: 160 °C, 0.1 M reactant solution, microreactor length of 4.5 m, 40 mM $AlCl_3$ or 0.39 mM HCl (both yielding pH = 3.4 at 20 °C), 4:1 organic to aqueous inlet flow ratio.

When using HMF as the substrate and $AlCl_3$ as the catalyst (pH = 3.4 at 20 °C), the HMF conversion, FA and LA yields were 10.8%, 13%, and 5% at a residence time of 20 min in the microreactor, respectively (Fig. 4.4 a). These values are considerably higher than experiments with HCl only (2.6%, 1.3% and 0.2%, respectively; Fig. 4.4 b). This implies that Al species, beside H^+, catalyzes the conversion of HMF[24]. In both cases, the observed stoichiometric excess of FA relative to LA is believed to originate from other reaction route(s) (e.g., from the direct degradation of HMF or from the oxidation of HCHO via HMF decomposition[24,53,54]; Fig. 4.3). The carbon balance in both cases became worse at increasing HMF conversion, owing to

the more significant generation of the unidentified product (e.g., oligomers or humins; Fig. 4.3).

4.3.2.2. Experiments with fructose

When using fructose as the substrate and $AlCl_3$ as the catalyst (Fig. 4.5 a), the fructose conversion reached 97.3% at 20 min in the microreactor with an HMF yield of 34% and an FA yield of 118%. Glucose and mannose were already formed at an early stage of the reaction (the respective yields reaching a maximum of 13.3% and 11.7% at 2 min). In the presence of HCl (Fig. 4.5 b), the fructose conversion (14.7% at 20 min) is by far lower than with $AlCl_3$. The corresponding HMF yield was 5.1% (and 6.9% for FA), whereas small amounts of glucose and mannose were formed (1.6% and 1.2% in yield, respectively). In another control experiment starting from fructose without catalyst under the same operating conditions, similar glucose and mannose yields were obtained (1.5% and 1.3% at 20 min, respectively). This implies that the reversible isomerization between fructose and glucose or mannose (and possibly the epimerization between glucose and mannose) is catalyzed mainly by Al species and only in very minor amounts by H^+. Besides, the higher fructose conversion and product yields in $AlCl_3$-catalyzed case is possibly due to a higher activity of the active Al species than that of HCl. In both cases (particularly for $AlCl_3$), more FA than LA was observed. Besides, the FA formation already started at an early stage of the reaction, when the HMF yields were still low. Thus, both $AlCl_3$ and HCl catalyze the direct degradation of fructose to FA, in line with the literature[24,49]. The FA yields are even higher than 100% (Fig. 4.5 a), which implies that one fructose molecule decomposes to more than one FA molecule. In both cases, the carbon balance became worse with increasing fructose conversion, indicating the gradual formation of the unidentified byproducts (accompanying the FA formation) (cf. Fig. 4.3).

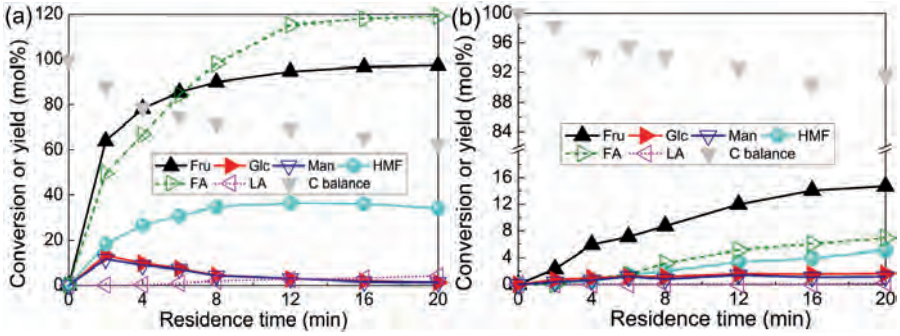

Fig. 4.5. Results of experiments with fructose as the substrate in a biphasic system in the slug flow capillary microreactor with (a) $AlCl_3$ and (b) HCl as catalyst. Other reaction conditions are the same as those specified in Fig. 4.4.

4.3.2.3. Experiments with glucose

For experiments with glucose as the substrate and $AlCl_3$ as the catalyst (Fig. 4.6 a), fructose and mannose were initially formed (mainly derived from the isomerization and epimerization of glucose, respectively[17]), and then consumed rapidly to give HMF or byproducts such as humins, together with a large amount of FA. The HMF yield increased gradually with the glucose conversion reaching a maximum of 35% at 16 min, followed by a slight decrease to 29% (at 20 min) due to its further degradation or oligo-polymerization to byproducts[8]. In the presence of HCl as catalyst (Fig. 4.6 b), the glucose conversion was rather low (ca. 10% at 20 min), and limited amounts of fructose, mannose, HMF and FA (the respective yields up to 1.5%, 0.6%, 0.3% and 2%) as well as a trace amount of LA were observed. Higher HMF yields obtained in the $AlCl_3$-catalyzed are highly likely due to the much higher isomerization activity of Al species than HCl (*vide supra*) to fructose and the higher rates of HMF formation from fructose (*vide supra*). The gradual decrease of carbon balance with increasing glucose conversion in both cases could be similarly explained by the side reactions involving sugars and HMF (cf. Fig. 4.3)[24,55], as discussed above.

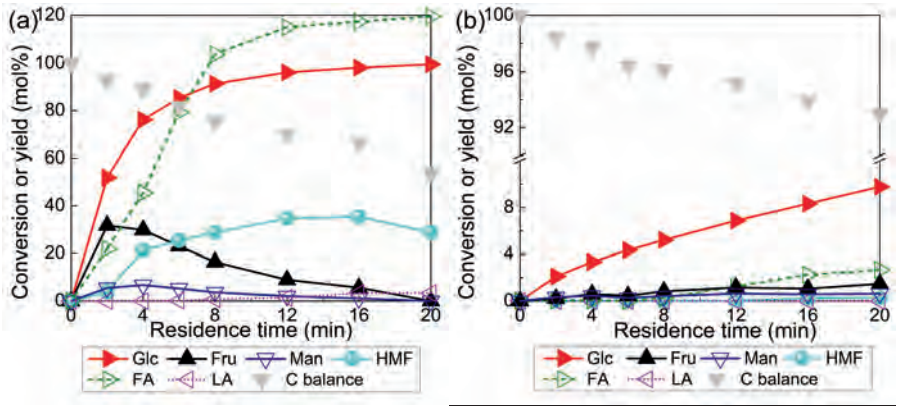

Fig. 4.6. Results of experiments with glucose as the substrate in a biphasic system in the slug flow capillary microreactor with (a) $AlCl_3$ and (b) HCl as catalyst. Other reaction conditions are the same as those specified in Fig. 4.4.

4.3.2.4. Role of the individual catalyst component

The above experiments starting from HMF, fructose and glucose using either $AlCl_3$ or HCl as catalyst (under the same pH value measured at ca. 20 ^{o}C), combined with the literature results[16,24,30,45], provide valuable insights in the roles of Al species and Brønsted acidity in the glucose conversion network (Fig. 4.7). In summary, the reversible isomerization of glucose to fructose and epimerization of glucose to mannose are catalyzed mainly by Al species, while the subsequent fructose dehydration to HMF as well as HMF rehydration to FA and LA is catalyzed by both, though higher rates were observed with Al species under the prevailing conditions. Besides, both Al species and HCl catalyze side reactions involving glucose, fructose and HMF, such as their degradation to FA and polymerization to humins.

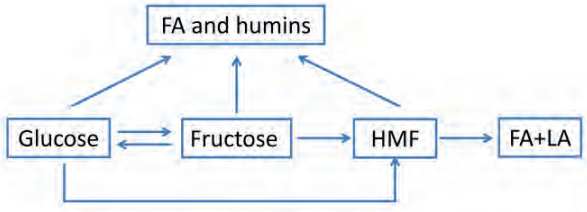

Fig. 4.7. Simplified view of the main reaction routes during HMF synthesis from glucose (based on the details depicted in Fig. 4.3).

4.3.3. Effect of Brønsted acidity on the $AlCl_3$/HCl-catalyzed glucose conversion in the slug flow capillary microreactor

As elaborated in Section 4.3.2, both $AlCl_3$ and HCl play a catalytic role in different reactions in the glucose conversion network. Thus, fine tuning the ratios of HCl and $AlCl_3$ is an important optimization tool to improve the HMF yield (in the current microreactor system) as well as to gain a better understanding into the effects of the different catalyst components in the reaction network (Fig. 4.7). It is noteworthy that the synthesis of HMF from glucose using the combined $AlCl_3$ and HCl as catalyst has been briefly demonstrated by Pagán-Torres et al.[11]. However, a more systematic investigation into the effect of Brønsted acidity on regulating the glucose conversion network as well as mechanisms thereof is still lacking. Additional experiments on the glucose conversion in the slug flow capillary microreactor were thus conducted, where Brønsted acidity of the reaction medium was adjusted (within a pH range of 0-4) by the addition of HCl at a fixed $AlCl_3$ concentration in the aqueous phase. Experiments were conducted at three $AlCl_3$ concentration levels (10, 20 and 40 mM) and the results are given in Fig. 4.8. Similar profiles for the glucose conversion, product yields and carbon balance with respect to the pH values were observed. Clearly, three regimes can be discriminated: 2< pH <4, 1< pH <2 and pH <1.

4.3.3.1. Regime 1 (2 < pH <4)

In this regime, the glucose conversion and fructose yield were about constant (Figs. 4.8 a and b). This suggests the presence of a rapid isomerization equilibrium between glucose and fructose, supported by the constant concentration ratio of fructose to glucose in this range. The ratio is close to 1.9, which is the equilibrium value as reported in the literature[46,47]. It implies that the subsequent conversions of fructose (e.g. to HMF) are slow compared to the isomerization, likely due to the low Brønsted acidity in this regime. Besides, the LA yield was almost constant in this regime and less than 3% (Fig. 4.8 d). As such, the rate of the HMF rehydration in this regime is low, supported by the results of the control experiments using HMF as the substrate (cf. Fig. 4.4). A different profile was found for FA (Fig. 4.8 c). Here, high amounts were formed at the highest pH value in this regime. It implies that the FA formation was mainly from $AlCl_3$-catalyzed degradation of sugars and/or HMF, as also supported by the literature observation (e.g., FA with a yield over 100% was obtained from glucose under the catalysis of $AlCl_3$ only[24]). As a result, the HMF yield went up (Fig. 4.8 e) and the carbon balance

was improved with the pH decrease (Fig. 4.8 f).

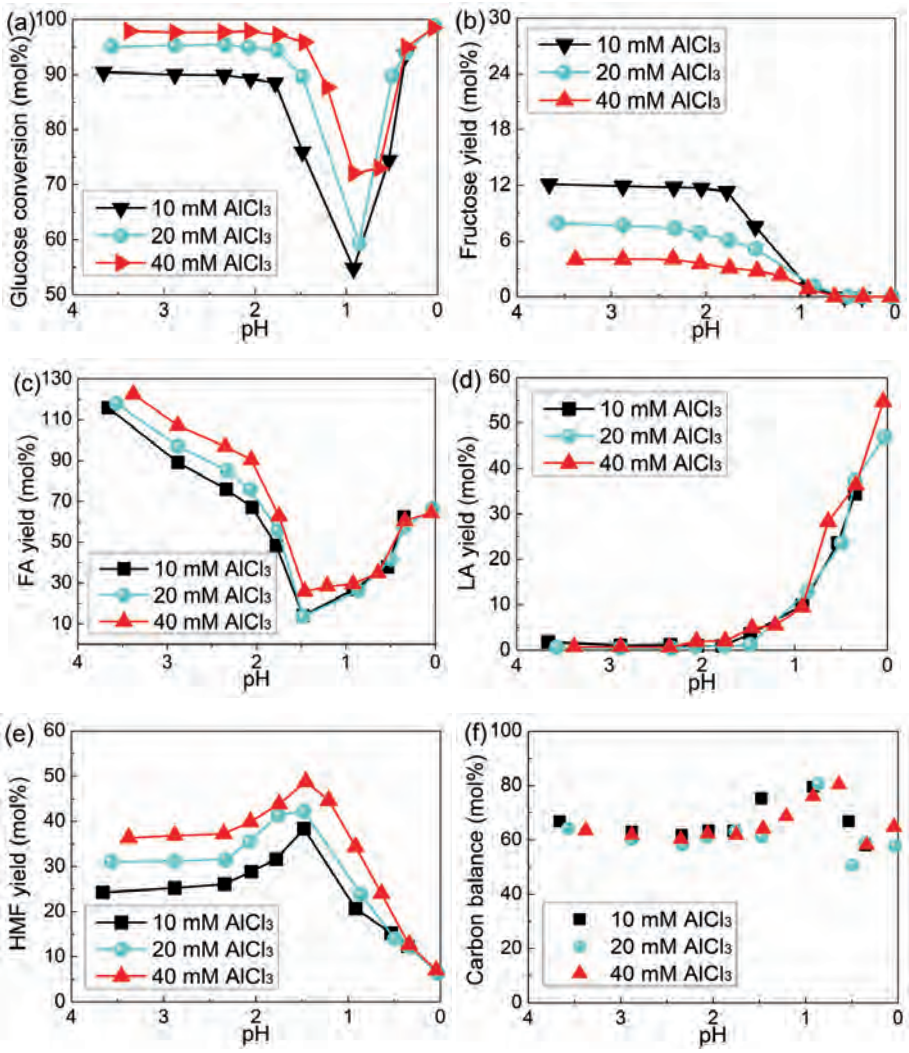

Fig. 4.8. Effect of Brønsted acidity on the glucose conversion reaction performance in the slug flow capillary microreactor using $AlCl_3$ and HCl as catalyst. (a) glucose conversion; (b) fructose yield; (c) FA yield; (d) LA yield; (e) HMF yield; (f) carbon balance. Other reaction conditions: 0.1 M glucose, 160 °C, microreactor length of 4.5 m, residence time at 16 min, 4:1 organic to aqueous inlet flow ratio, pH values were adjusted by the addition of HCl in the aqueous phase and reported according to the measurement at ca. 20 °C.

4.3.3.2. Regime 2 (1< pH <2)

In this regime, the glucose conversion showed a sharp drop, with a minimum at a pH value of about 1. This trend is also visible for the fructose yield, which dropped to almost zero (Figs. 4.8 a and b). The concentration ratios of fructose to glucose were much lower than 1.9, suggesting that the glucose isomerization to fructose was not at equilibrium[46,47]. This is due to: i) a gradual shift of $AlCl_3$ hydrolysis equilibrium at higher Brønsted acidity with less active Al species present, leading to a lower rate of the glucose isomerization (and a longer time needed to reach equilibrium); ii) a faster fructose dehydration to HMF and/or other byproducts (such as FA and humins) than its isomerization to glucose, which is facilitated by the significantly increased Brønsted acidity[48]. The FA yield showed a steady decline until pH = 1.5 and then increased again upon a further reduction of the pH (Fig. 4.8 c). At pH > 1.5, the FA formation was mainly from sugar or HMF degradation catalyzed by Al species and suppressed with the pH decrease due to less catalytic Al species available. At pH < 1.5, HCl-catalyzed FA formation, from either the rehydration of HMF or the degradation of sugars or HMF, became more prevalent with a further pH decrease. In the 1 < pH < 2 regime, the LA yield increased gradually with decreasing pH value (Fig. 4.8 d). The conversion of HMF to LA is highly sensitive to the pH of the solution with increasing Brønsted acidity leading to higher rates, as kinetic studies have indicated a reaction order close to unity (with respect to H^+) for the HMF rehydration under acidic conditions[8,48,55-57].

The HMF yield trend was exactly opposite to that of FA (Fig. 4.8 e). A maximum HMF yield was found at about pH = 1.5. At pH > 1.5, the fructose dehydration to HMF was improved with decreasing pH, supported by the suppression of the reactions of fructose to byproducts (among others FA and the unidentified humins, cf. Figs. 4.8 c and f). At pH < 1.5, the HMF rehydration to LA and degradation to byproducts were more significant with increasing pH [8,48,55-57] (cf. Figs. 4.8 d and f).

In the range of 1 < pH < 4 (i.e., regimes 1 and 2), a higher $AlCl_3$ concentration generally led to higher glucose conversion and yields of fructose, FA and HMF (Figs. 4.8 a-c and e). This result is further supported by additional glucose conversion experiments conducted in a biphasic system in the microreactor at 160 °C with $AlCl_3$ concentrations up to 80 mM in the presence of HCl to maintain a constant pH (cf. Fig. S4.4 in the Supplementary material), except the additional observation that the HMF yield at a residence time of 16 min declined from its

maxima (at ca. 40 mM $AlCl_3$) upon further increasing the $AlCl_3$ concentration. Such yield decline may be due to the more significant side reactions catalyzed by $AlCl_3$ such as the HMF degradation to FA and polymerization to humins[24] (Figs. 4.3 and 4.7).

4.3.3.3. Regime 3 (pH < 1)

In this regime, the glucose conversion increased dramatically when lowering the pH (Fig. 4.8 a). However, the yield of fructose showed a clear reduction and nearly no fructose was detected at pH < 0.5 (Fig. 4.8 b). Meanwhile, the yields of FA and LA increased sharply (Figs. 4.8 c and d), and the HMF yield declined (to about 5% at pH = 0; Fig. 4.8 e). These yield trends with the pH are explained by a major effect of Brønsted acidity on the rates of the relevant individual reactions. The increase in the glucose conversion at lower pH values is likely due to a rapid increase in the HCl-catalyzed conversions of glucose to HMF and byproducts like FA and humins (Figs. 4.3 and 4.7)[18], with a reduction in the isomerization activity due to the formation of Al species at lower pH values that are less active isomerization catalysts. To examine the contribution of the former route, control experiments with glucose as the substrate and HCl as the catalyst at different pH values (without the addition of $AlCl_3$) were conducted under otherwise the same reaction conditions in the microreactor (see Fig. S4.5 in the Supplementary material for the results). The glucose conversion was constant at around 9% for pH values between 1.5 and 3.4. However, a gradual increase when lowering the pH below 1.5 was visible, and 89% conversion was found at pH = 0.3. The HMF yield was 11.4%, in line with the literature kinetic studies showing that the direct glucose conversion to HMF is very unselective[18,55,56]. Notably, a similar HMF yield was obtained (12.7%) when using a combination of $AlCl_3$ (40 mM) and HCl as catalysts at the same pH (Fig. 4.8 e). Moreover, Figs. 4.8 b-e show no distinct differences in the product yields for the three different $AlCl_3$ concentrations at pH < 1. As such, in this regime, Brønsted acidity is by far more important than catalysis by Al species.

In summary, the results show that the highest HMF yield is possible when using a catalyst mixture consisting of 40 mM $AlCl_3$ and 40 mM HCl (with pH = 1.5 at ca. 20 °C). At these conditions, a proper balance between Brønsted acidic HCl and Lewis acidic Al species exists to enhance the rate of reactions leading to HMF while suppressing the formation of FA, LA and other byproducts. In the regime of 2 < pH < 4, Al species mainly play the catalytic role, with

the presence of high glucose isomerization activity and limited fructose dehydration rate. In the intermediate regime of 1< pH < 2, both Al species and HCl catalyze the reactions, with the presence of a significant conversion of glucose to HMF via fructose. In the regime of pH < 1, HCl plays mainly the catalytic role, with low yields of HMF derived mainly from the direct, but unselective glucose dehydration.

4.3.4. Further Insights into the variation of the catalytically active Al species with Brønsted acidity and the pH dependency of the glucose conversion

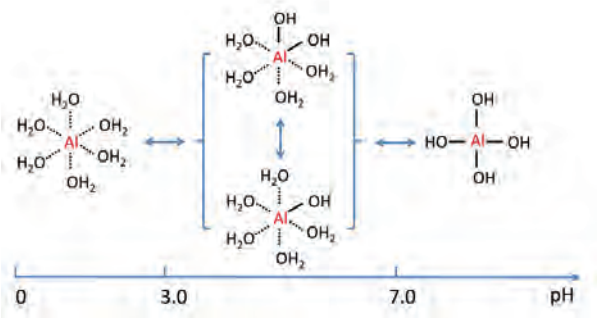

Fig. 4.9. Schematic representation of Al (III) cations in water under different Brønsted acidities.

In order to further elucidate the pH dependency of the glucose conversion and HMF yield, it is necessary to inversigate the variation of the catalytically active Al species with pH. It is well established that metal ions play a major role in the conversion of glucose to HMF. For instance, many metals (such as Cr^{3+}, Zn^{2+}, Sn^{4+} and Al^{3+}) catalyze the isomerization of glucose to fructose[11,15,16,24,29,30]. However, it is often difficult, particularly in water, to identify the catalytically active species. One of the reasons is the presence of a number of metal species in water, often in equilibrium with each other of which the amount depends on the pH and temperature. For instance, in water at room temperature, Al^{3+} can be present in the form of: i) hexa-coordinated $[Al(H_2O)_6]^{3+}$ at pH < 3; ii) hexa-coordinated monomers like $[Al(OH)_2(H_2O)_4]^+$ and $[Al(OH)(H_2O)_5]^{2+}$, dimers like $[Al_2(OH)_2(H_2O)_8]^{4+}$, etc. at pH = 3 - 7; and iii) tetra-coordinated $[Al(OH)_4]^-$ together with some polymers in the basic solution[32,58], as shown in Fig. 4.9. Choudhary et al.[17] found that Al^{3+} and $Al(OH)^{2+}$ are the dominant species in the $AlCl_3$ speciation via a Car-Parrinello molecular dynamics (CPMD) simulation, and $Al(OH)^{2+}$ was

predicted to be the catalytically active species for the glucose isomerization to fructose. Tang et al.[24,59] observed the coordination between the glucose molecule and $Al(OH)^{2+}$ species via ESI-MS spectra, and postulated that the main catalytically active species for the glucose isomerization reaction was most possibly $Al(OH)^{2+}$. However, both cases focused on the glucose isomerization, without presenting a more detailed study on the pH dependency of the catalytically active species and the relevant effect on the subsequent fructose dehydration to HMF as well as other side reactions.

4.3.4.1. ESI-MS/MS characterization of the aqueous glucose solutions with $AlCl_3$ and HCl

To gain insights into the variation of the active Al species with Brønsted acidity during the glucose conversion, the aqueous glucose solutions containing HCl (40 or 640 mM) and/or $AlCl_3$ (40 mM) were prepared and characterized by ESI-MS/MS (Fig. 4.10). Peaks of $[Al(OH)_2+(Glc)-H_2O]^+$, $[Al(OH)_2+(Glc)]^+$ and $[Al(OH)_2+2(Glc)-2H_2O]^+$ fragments (at m/z = 223, 241 and 385, respectively) are present in the ESI-MS spectra of all samples (Figs. 4.10 a-c). MS/MS was further performed on the selected peak at m/z=385 (Fig. 4.10 d), then more peaks involving $[Al(OH)_2]^+$ species appeared, such as $[Al(OH)_2H_2O+(Glc)]^+$ and $[Al(OH)_2(H_2O)_2+(Glc)]^+$ at m/z = 259 and 277, respectively. These results indicate that $[Al(OH)_2]^+$ species are mainly present in the solution (e.g., at the optimized pH = 1.5) and form coordination complexes with glucose. Peaks corresponding to $[Al+(Glc)_n]^{3+}$, $[Al(OH)+(Glc)_n]^{2+}$ or $[Al(OH)_3+(Glc)+nH]^{n+}$ species were not detected. This suggests that the catalytically active species in the glucose conversion network is $[Al(OH)_2]^+$ species, which has also been observed in the work of Tang et al.[24,59] using only $AlCl_3$ as catalyst and is also in line with our experimental results on the pH dependency of the glucose conversion in the coexistence of additional HCl (Fig. 4.8). At lower pH values (e.g., < 3.4), the intensity of the peaks from glucose-coordinated $[Al(OH)_2]^+$ compounds (e.g. at m/z = 223, 241 and 385) was lowered gradually (Figs. 4.10 a-c), indicating that the amounts are a function of Brønsted acidity of the solution (see also Fig. 4.9).

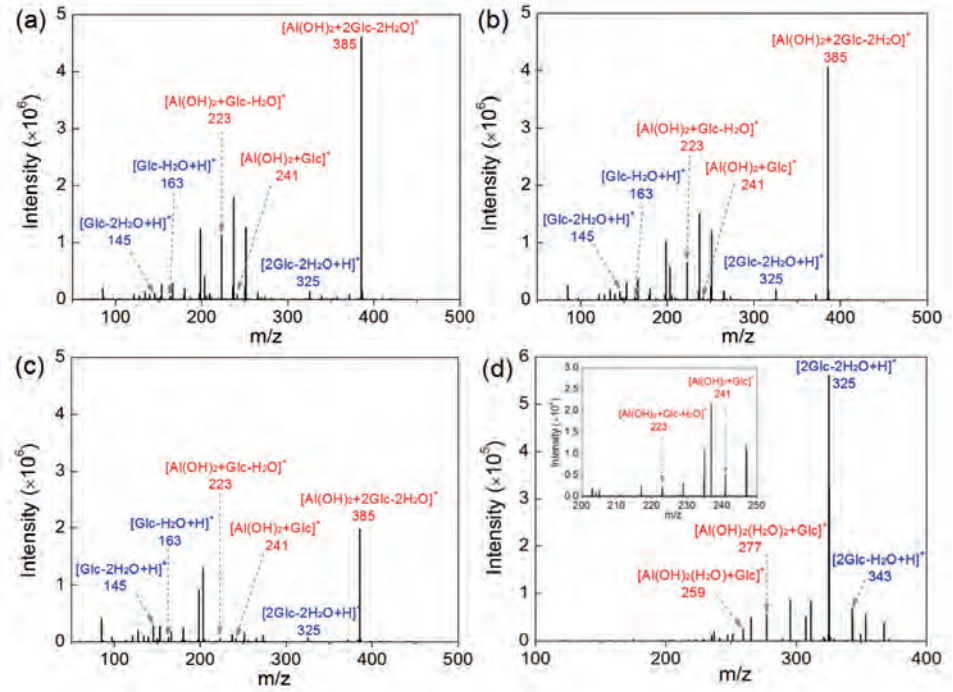

Fig. 4.10. ESI-MS spectra of the fresh aqueous 0.1 M glucose solution containing (a) 40 mM $AlCl_3$ (pH = 3.38); (b) 40 mM $AlCl_3$ and 40 mM HCl (pH = 1.5); (c) 40 mM $AlCl_3$ and 640 mM HCl (pH = 0.34); and (d) MS/MS spectra of the selected $[Al(OH)_2+2Glc]^+$ species of sample (b) with m/z of 385. Inset in (d) shows a magnified view of m/z region at 200-250.

4.3.4.2. ESI-MS characterization of the aqueous phase after reaction

The type and relative amounts of aluminum coordination compounds after the reaction were investigated by analyzing the aqueous product samples collected from a typical microreactor experiment (0.1 M glucose, 40 mM $AlCl_3$ and 40 mM HCl (pH = 1.5) at 160 ^oC and 4 min and 16 min residence times) using ESI/MS. The results for an experiment at a residence time of 4 min are shown in Fig. 4.11 a. Distinct peaks are present at m/z= 223, 241 and 385, in line with the model experiments with the aqueous glucose solutions (*vide supra*). These peaks are assigned to, respectively, $[Al(OH)_2+C6sugar-H_2O]^+$, $[Al(OH)_2+C6sugar]^+$ and $[Al(OH)_2+2C6sugar-2H_2O]^+$, where the sugar is either glucose, mannose or fructose. In addition, some peaks related to the presence of HMF are present (at m/z=109 and 137). At an extended residence time (16 min; Fig. 4.11 b), the peak intensities of the C6 sugar and HMF coordinated

$[Al(OH)_2]^+$ compounds are different from the ones at lower residence times. The former ones have increased and the latter decreased, in line with a higher glucose conversion at longer residence times. In addition, additional peaks assigned to $[C6sugar+H-2H_2O-FA]^+$ at m/z=99 and $[Al(OH)_2+C6sugar-FA]^+$ at m/z=195 were present. This suggests that the FA may be formed directly from fructose and/or glucose[24]. Besides, a peak at m/z = 157 is observed, which may be from $[Al(OH)_2+HMF-HCHO]^+$, which is indicate of the HMF reaction under these conditions to give furfural and formaldehyde[24]. The former was indeed also observed in the spectrum (at m/z=97; Fig. 4.11 b). Formaldehyde may be a precursor to FA by oxidation with air[24]. The peak at m/z=69 corresponds to furan, which may be formed (together with FA) via the hydrolysis of furfural[53,54]. Thus, the ESI-MS data support the reaction network as detailed in Fig. 4.3.

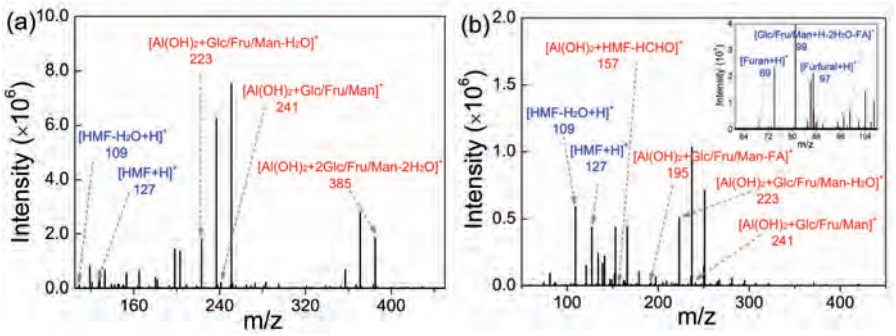

Fig. 4.11. ESI-MS spectra of the aqueous product sample collected after the reaction of 0.1 M glucose solution containing 40 mM $AlCl_3$ and 40 mM HCl (pH = 1.5 measured at ca. 20 °C) in the microreactor for a residence time of (a) 4 min and (b) 16 min. Inset in (b) shows a magnified view of m/z region at 80-108. Other reaction conditions: 160 °C, microreactor length of 4.5 m, 4:1 organic to aqueous inlet flow ratio.

4.3.5. Further screening of the reaction conditions for optimized HMF yield

To further explore the potential of microreactor operation in the HMF synthesis, additional experiments have been conducted to study the effect of parameters including the reaction temperature (T), the glucose concentration ($C_{aq,Glc,0}$), the extraction solvent type, the organic to aqueous volumetric flow ratio (Q_{org}/Q_{aq}) and the addition of salt on the reaction performance in terms of the glucose conversion (X_{Glc}) and the HMF yield (Y_{HMF}). Best HMF yields under different conditions are briefly summarized in Table 4.1.

Table 4.1. Influence of the reaction conditions on the glucose conversion and HMF yield.[a]

Entry	T (°C)	τ (min)	$C_{aq,Glc,0}$ (M)	Organic solvent	Q_{org}/Q_{aq} (-)	$C_{aq,NaCl,0}$[b] (wt%)	X_{Glc} (mol%)	Y_{HMF} (mol%)
1	150	20	0.1	MIBK	4:1	0	87.7	41.7
2	160	12	0.1	MIBK	4:1	0	88.0	50.9
3	160	16	0.1	MIBK	4:1	0	95.8	53.0
4	170	16	0.1	MIBK	4:1	0	97.4	48.8
5	160	12	0.1	MIBK	2:1	0	96.7	46.5
6	160	8	0.1	MIBK	1:1	0	90.6	40.7
7	160	16	0.3	MIBK	4:1	0	94.2	53.9
8	160	16	0.1	MIBK	4:1	5	89.4	59.8
9	160	16	0.1	MIBK	4:1	10	83.7	60.4
10	160	16	0.1	mTHF	4:1	0	96.4	66.4
11	160	16	1.0	MIBK	4:1	20	83.2	66.2

[a] Other reaction conditions: microreactor length of 4.5 m, 40 mM $AlCl_3$ and 40 mM HCl (pH = 1.5 measured at 20 °C); [b] NaCl concentration in the aqueous feed.

Temperature plays an important role in adjusting the kinetic behavior of the glucose conversion (Entries 1-4; Table 4.1), that is, the relative rates of the reactions in the glucose conversion network including HMF synthesis as well as side reactions such as humin formation and HMF rehydration (cf. Figs. 4.3 and 4.7). A reaction temperature of 160 °C was found optimal, with a high organic to aqueous volumetric flow ratio (e.g., at 4:1) preferred for obtaining a high HMF yield (Entries 3, 5 and 6; Table 4.1), as more HMF would be extracted thus being prevented from its degradation in side reactions in the aqueous phase. The influence of the glucose concentration on the HMF yield turned out to be limited (Entries 3 and 7 in Table 4.1; cf. Fig. S4.6 in the Supplementary material as well), indicating an overall first-order reaction with respect to glucose regarding the HMF formation. Besides, the HMF yield could be further improved by enhancing the partition of HMF into organic phases, via salting out effect by adding NaCl into the aqueous phase[25], or using a more capable (albeit expensive or toxic) organic solvent such as methyltetrahydrofuran (mTHF) and 2-sec-butyl phenol[39]. For instance, Table 4.1 shows that the HMF yield was promoted from 53% to 60.4% if 10 wt% NaCl was added in the water/MIBK biphasic system (Entries 3 and 9), and to 66.4%

with mTHF as the extraction solvent (Entry 10). Under the investigated conditions, a further optimized HMF yield of 66.2% was achieved in the water/MIBK biphasic system using a concentrated 1.0 M glucose feedstock solution with the presence of 20 wt% NaCl, at 160 °C and Q_{org}/Q_{aq} of 4:1, and a short residence time of 16 min (Entry 11).

4.3.6. Performance comparison of microreactors with a laboratory batch reactor study and the literature work

The experimental data for HMF synthesis from glucose in a water-MIBK biphasic system in the slug flow capillary microreactor were compared with those obtained in a laboratory batch reactor set-up (see Section S4.7 in the Supplementary information for the batch experiment details). The reaction rates appeared to be much higher in the microreactor than in batch (Fig. 4.12; 40 mM $AlCl_3$ and 40 mM HCl). The HMF yield reached 40.9% (at a glucose conversion of 81%) at 8 min in the microreactor while 16 min were required to reach an HMF yield of 38.0% (at a glucose conversion of 76%) in the batch reactor. Two factors are possible to explain these differences, viz. heating effect and mass transfer effect (related to the transfer of HMF from water to MIBK). Mass transfer limitation was excluded in the batch reactor under the operating conditions (i.e., at a stirring speed of 500 rpm), since no difference in either the glucose conversion or HMF yield was observed for a stirring speed above 400 rpm (cf. Fig. S4.8 in the Supplementary material). To prove whether heating effect played a major role, the heating profile of the batch reactor was measured (in the presence of an aqueous glucose solution and MIBK at an organic to aqueous volume ratio of 4:1) and that of the microreactor was estimated (for a simplified case of laminar flow of water or MIBK therein), as shown in Fig. S4.9 in the Supplementary material. In the microreactor, the feed could be heated to the target temperature of 160 ^{o}C within 20 s due to an excellent thermal management (e.g., by a very large specific surface area for heat transfer). However, it took over 5 minutes to reach this target temperature in the batch reactor, primarily due to its smaller surface to volume ratio compared with the microreactor leading to a lower heat transfer efficiency. Consequently, it is likely that the reaction rate in the batch reactor was slowed down due to an on average lower temperature in the reactor by a relatively slow heating profile.

A faster reaction rate in the microreactor also translates into an improved space time yield. Based on the results in Fig. 4.12, space time yields in the microreactor were calculated to be

from 351 to 1010 mmol HMF · m^{-3} · min^{-1}, which are on average much higher than those in the batch reactor of this work ranging from 188 to 438 mmol HMF · m^{-3} · min^{-1} (see Table S4.5 and the detailed calculation in Section S4.9 in the Supplementary material). The performance of the current microreactor system was also compared with some typical literature work that reported higher HMF yields in either batch reactors or microreactors using homogeneous or solid acid catalysts [17,39,60-62]. The current microreactor affords a much higher or at least comparable space time yield of HMF (cf. Table 4.2). It is noted that the HMF yield was almost constant with increasing glucose concentration (e.g., from 0.1 to 0.3 M; cf. Table 4.1 and Fig. S4.6 in the Supplementary information) in the current microreactor due to approximately an overall first-order reaction with respect to glucose regarding HMF formation, and thus the space time yields of HMF could be further increased substantially by processing in the current microreactor using more concentrated feedstock. For example, the optimized HMF space time yield obtained from 1 M glucose feedstock solution (Table 4.2) turned out to be as high as 7031.8 mmol · min^{-1} · m^{-3}.

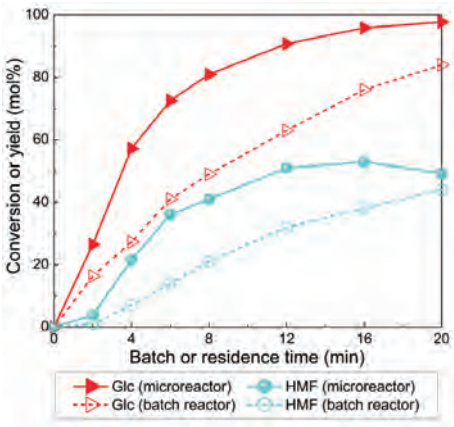

Fig. 4.12. Glucose conversion and HMF yield as a function of the residence time in the microreactor and the batch time in the batch reactor in a biphasic system at optimized conditions. Reaction conditions: 0.1 M glucose, 160 °C, 40 mM $AlCl_3$ and 40 mM HCl (pH = 1.5 measured at ca. 20 °C), organic to aqueous inlet flow ratio or initial volume ratio at 4 : 1.

Table 4.2. Comparison of the HMF space time yield from glucose in a biphasic water-organic solvent system in the current microreactor with the literature results.

Catalyst	Organic solvent	Reactor type	*T* (°C)	Time[a] (min)	Y_{HMF} (mol%)	Space time yield (mmol HMF·min^{-1}·m^{-3})	Work
Phosphate buffer saline	MIBK	Slug flow microreactor	180	47	75.7	226	[39]
$CrCl_3$/HCl	THF[b]	Batch reactor	140	180	59	612	[17]
Phosphated titania	THF	Batch reactor	105	175	83.4	178	[60]
Nb-Beta zeolite	MIBK[b]	Batch reactor	180	720	82.1	22.8	[61]
Seawater (30 wt% NaCl)	THF	Batch reactor	200	360	48.6	28.2	[62]
$AlCl_3$/HCl	mTHF[c]	Slug flow microreactor	160	16	66.4	705.3	This work
$AlCl_3$/HCl	MIBK[c]	Slug flow microreactor	160	16	53	510.3	This work
$AlCl_3$/HCl	MIBK[b,d]	Slug flow microreactor	160	16	66.2	7031.8	This work

[a] Reaction time in the batch reactor or residence time in the microreactor; [b] With the addition of 20 wt% NaCl in the aqueous phase; [c] With 0.1 M glucose feedstock solution; [d] With 1 M glucose feedstock solution.

It is well known that batch reactors for carrying out reactions in biphasic systems usually suffer from poor flow pattern control and mixing when scaled up, which implicates that for HMF synthesis the low mass transfer efficiency therein tends to limit the HMF extraction and leads to low HMF yields. To further determine whether there was a mass transfer limitation in the microreactor, the glucose conversion experiments were performed in the slug flow capillary microreactors of different lengths (L_C; being 1.2, 4.5 and 17 m) under the same 8 min residence time. A higher flow rate (or equivalently, higher droplet/slug velocity) is known to enhance internal circulation leading to higher mass transfer rates[34-36,41]. As such, a significantly higher HMF yield is expected in a much longer microreactor in the presence of

mass transfer limitation. However, as shown in Fig. 4.13, product yield differences (including those of HMF) are only minor among microreactors of different lengths, indicating that mass transfer resistance was entirely or at least largely eliminated in microreactors and the reaction was performed (largely) in the kinetic regime.

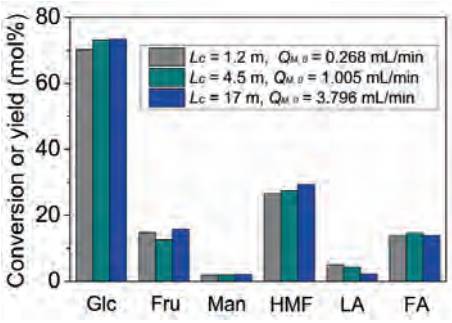

Fig. 4.13. Glucose conversion and product yields in the slug flow capillary microreactor of different lengths. Reaction conditions: 0.1 M glucose, 160 °C, 40 mM $AlCl_3$ and 40 mM HCl (pH = 1.5 measured at ca. 20 °C), 8 min residence time, 4 : 1 organic to aqueous inlet flow rate ratio. In the legend, $Q_{M,0}$ represents the total volumetric flow rate of the two-phase mixture at the microreactor inlet.

In summary, the application of slug flow capillary microreactors for HMF synthesis provides superior heat and mass transfer efficiencies, as compared with the batch reactor (especially when scaled-up). Thus, microreactor processing largely facilitates the reaction to run in the kinetic regime under isothermal conditions, and allows to obtain a higher HMF yield by enhanced HMF extraction to the organic phase. In addition, the current microreactor system has advantages such as continuous flow mode, the direct numbering-up approach for a fast product capacity increase [63] and thereby represents a promising reactor type for potential industrial application.

4.3.7. Recyclability and reusability of the $AlCl_3$/HCl catalyst system

Recyclability and reusability of the current homogeneous $AlCl_3$/HCl catalyst system are important from the perspective of industrial application, an aspect that has not been examined so far. To evaluate this, a number of recycle runs were performed where the aqueous phase (with the catalyst) after a biphasic reaction in the microreactor (at 16 min residence time) was collected and reused for the reaction test in a next run (Fig. 4.14). For a

proper comparison, HMF as well as other byproducts (such as FA and LA) in the aqueous phase was largely removed via multiple (at least 3) batch extraction with MIBK (using 4:1 organic to aqueous volume ratio). In addition, a filtration step was followed in order to remove insoluble humins (actually little solid humin was observed under these conditions). Fig. 4.14 shows that the catalyst performance for three successive runs in the microreactor at the optimized reaction conditions using 0.1 M glucose solution as the feedstock. The glucose conversion and yields of HMF as well as other products were very similar for all runs, indicating a good stability and recyclability of the $AlCl_3$/HCl catalyst system. From the ICP-AES results (not shown for brevity), no Al species were detected in neither the recycled MIBK phase after the $AlCl_3$/HCl-catalyzed glucose conversion, nor the fresh MIBK phase after pretreatment by mixing with the $AlCl_3$ solution. Thus, the good catalyst stability is primarily due to no appreciable Al species loss in terms of either precipitation in the aqueous phase or transferring to the MIBK phase during the glucose conversion reaction under the investigated conditions.

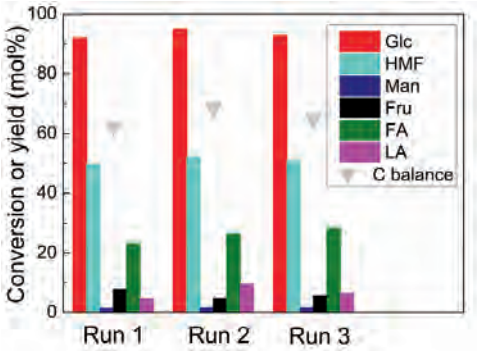

Fig. 4.14. Evaluation of the reusability of the combined $AlCl_3$/HCl catalyst in the glucose conversion in the slug flow capillary microreactor at the optimized reaction conditions using 0.1 M glucose solution as the feedstock (as those shown in Fig. 4.2).

4.4. Conclusion

An experimental study on HMF synthesis from glucose in a biphasic system was performed in a capillary microreactor operated under slug flow, using the homogeneous $AlCl_3$/HCl catalyst in the aqueous phase and MIBK as the organic phase for in-situ HMF extraction. After optimization, an HMF yield of 53% was achieved at 160 °C within a residence time of 16

minutes in the microreactor in the presence of 40 mM $AlCl_3$ and 40 mM HCl (pH = 1.5 measured at 20 ^oC). The HMF yield could be further increased to over 66% by enhancing the HMF extraction into the organic phase, i.e., by either adding 20 wt% NaCl in the aqueous phase or using mTHF as the extraction solvent. Under the above optimized catalyst combinations, Brønsted and Lewis acidities of the aqueous reaction medium were regulated such that the prevalent reaction route was driven towards the reversible glucose isomerization to fructose (catalyzed by Al species) followed by the fructose dehydration to HMF (catalyzed by HCl), whereas the side reactions from glucose/fructose/HMF were largely suppressed (e.g., for the formation of formic acid, levulinic acid and humins; catalyzed by both Al species and HCl). This is further supported by the ESI-MS/MS characterization results which revealed $[Al(OH)_2]^+$ as most possibly the active Al species. Thus, by altering the Brønsted acidity (i.e., HCl addition), the $AlCl_3$ hydrolysis equilibrium and $[Al(OH)_2]^+$ concentration in water may be tuned to optimize HMF yields from glucose (via fructose). The aqueous catalytic phase was recycled and reused three times without noticeable performance loss, supported by no Al species losses via either dissolving into MIBK or precipitation in the aqueous solution. Compared with a laboratory batch reactor study, the current microreactor allowed a better temperature regulation (due to its excellent heat transfer efficiency), and therefore a faster reaction rate and a higher HMF yield. The optimized HMF space time yield in this work (using 1 M glucose solution as the feedstock) is also significantly higher than those in the literature work. In addition, the reaction in the microreactor has been shown to run (largely) under kinetic control, given that slug flow operation greatly promoted mixing/reaction in the aqueous droplet and facilitated HMF extraction to the organic slug for an enhanced HMF yield. The confinement of reaction in the aqueous droplets prevented humin deposition on the microreactor wall. Thus, continuous biphasic operation in microreactors, combined with the recyclable and stable homogenous $AlCl_3$/HCl catalyst, holds great promises for a more efficient and sustainable HMF synthesis from glucose.

References

1. van Putten, R.-J.; van der Waal, J. C.; de Jong, E.; Rasrendra, C. B.; Heeres, H. J.; de Vries, J. G., Hydroxymethylfurfural, a versatile platform chemical made from renewable resources. *Chem. Rev.* 2013, *113* (3), 1499-1597.

2. Rosatella, A. A.; Simeonov, S. P.; Frade, R. F. M.; Afonso, C. A. M., 5-Hydroxymethylfurfural (HMF) as a building block platform: Biological properties, synthesis and synthetic applications. *Green Chem.*

2011, *13* (4), 754-793.

3. Kong, X.; Zhu, Y.; Fang, Z.; Kozinski, J. A.; Butler, I. S.; Xu, L.; Song, H.; Wei, X., Catalytic conversion of 5-hydroxymethylfurfural to some value-added derivatives. *Green Chem.* 2018, *20* (16), 3657-3682.

4. Yan, D.; Xin, J.; Shi, C.; Lu, X.; Ni, L.; Wang, G.; Zhang, S., Base-free conversion of 5-hydroxymethylfurfural to 2,5-furandicarboxylic acid in ionic liquids. *Chem. Eng. J.* 2017, *323*, 473-482.

5. Gandini, A.; Silvestre, A. J.; Neto, C. P.; Sousa, A. F.; Gomes, M., The furan counterpart of poly (ethylene terephthalate): An alternative material based on renewable resources. *J. Polym. Sci., Part A: Polym. Chem.* 2009, *47* (1), 295-298.

6. Hu, L.; Li, T.; Xu, J.; He, A.; Tang, X.; Chu, X.; Xu, J., Catalytic transfer hydrogenation of biomass-derived 5-hydroxymethylfurfural into 2,5-dihydroxymethylfuran over magnetic zirconium-based coordination polymer. *Chem. Eng. J.* 2018, *352*, 110-119.

7. Román-Leshkov, Y.; Barrett, C. J.; Liu, Z. Y.; Dumesic, J. A., Production of dimethylfuran for liquid fuels from biomass-derived carbohydrates. *Nature* 2007, *447* (7147), 982.

8. Girisuta, B.; Janssen, L. P. B. M.; Heeres, H. J., A kinetic study on the decomposition of 5-hydroxymethylfurfural into levulinic acid. *Green Chem.* 2006, *8* (8), 701-709.

9. Alonso, D. M.; Wettstein, S. G.; Dumesic, J. A., Gamma-valerolactone, a sustainable platform molecule derived from lignocellulosic biomass. *Green Chem.* 2013, *15* (3), 584-595.

10.Dutta, S.; Yu, I. K. M.; Tsang, D. C. W.; Ng, Y. H.; Ok, Y. S.; Sherwood, J.; Clark, J. H., Green synthesis of gamma-valerolactone (GVL) through hydrogenation of biomass-derived levulinic acid using non-noble metal catalysts: A critical review. *Chem. Eng. J.* 2019, *372*, 992-1006.

11.Pagán-Torres, Y. J.; Wang, T.; Gallo, J. M. R.; Shanks, B. H.; Dumesic, J. A., Production of 5-hydroxymethylfurfural from glucose using a combination of lewis and brønsted acid catalysts in water in a biphasic reactor with an alkylphenol solvent. *ACS Catalysis* 2012, *2* (6), 930-934.

12.Angyal, S. J., The composition of reducing sugars in solution. *Adv. Carbohydr. Chem. Biochem.* 1984, *42*, 15-68.

13.Wang, T.; Glasper, J. A.; Shanks, B. H., Kinetics of glucose dehydration catalyzed by homogeneous Lewis acidic metal salts in water. *Applied Catalysis A: General* 2015, *498*, 214-221.

14.Zhang, X.; Hewetson, B. B.; Mosier, N. S., Kinetics of maleic acid and aluminum chloride catalyzed dehydration and degradation of glucose. *Energy & Fuels* 2015, *29* (4), 2387-2393.

15.Yang, Y.; Hu, C.-w.; Abu-Omar, M. M., Conversion of carbohydrates and lignocellulosic biomass into 5-hydroxymethylfurfural using $AlCl_3 \cdot 6H_2O$ catalyst in a biphasic solvent system. *Green Chem.* 2012, *14* (2), 509-513.

16.Swift, T. D.; Nguyen, H.; Anderko, A.; Nikolakis, V.; Vlachos, D. G., Tandem Lewis/Brønsted homogeneous acid catalysis: conversion of glucose to 5-hydoxymethylfurfural in an aqueous chromium (III) chloride and hydrochloric acid solution. *Green Chem.* 2015, *17* (10), 4725-4735.

17.Choudhary, V.; Mushrif, S. H.; Ho, C.; Anderko, A.; Nikolakis, V.; Marinkovic, N. S.; Frenkel, A. I.; Sandler, S. I.; Vlachos, D. G., Insights into the interplay of lewis and brønsted acid catalysts in glucose and fructose conversion to 5-(hydroxymethyl)furfural and levulinic acid in aqueous media. *J. Am. Chem. Soc.* 2013, *135* (10), 3997-4006.

18.Yang, Y.; Hu, C.; Abu-Omar, M. M., The effect of hydrochloric acid on the conversion of glucose to

5-hydroxymethylfurfural in $AlCl_3$ – H_2O/THF biphasic medium. *J. Mol. Catal. A: Chem.* 2013, *376*, 98-102.

19.Swift, T. D.; Nguyen, H.; Erdman, Z.; Kruger, J. S.; Nikolakis, V.; Vlachos, D. G., Tandem Lewis acid/Brønsted acid-catalyzed conversion of carbohydrates to 5-hydroxymethylfurfural using zeolite beta. *J. Catal.* 2016, *333*, 149-161.

20.Zhao, H.; Holladay, J. E.; Brown, H.; Zhang, Z. C., Metal chlorides in ionic liquid solvents convert sugars to 5-hydroxymethylfurfural. *Science* 2007, *316* (5831), 1597-1600.

21.Yong, G.; Zhang, Y.; Ying, J. Y., Efficient catalytic system for the selective production of 5-hydroxymethylfurfural from glucose and fructose. *Angew. Chem.* 2008, *120* (48), 9485-9488.

22.Nakajima, K.; Noma, R.; Kitano, M.; Hara, M., Selective glucose transformation by titania as a heterogeneous Lewis acid catalyst. *J. Mol. Catal. A: Chem.* 2014, *388* (Supplement C), 100-105.

23.Rasrendra, C.; Soetedjo, J.; Makertihartha, I.; Adisasmito, S.; Heeres, H., The catalytic conversion of d-glucose to 5-hydroxymethylfurfural in DMSO using metal salts. *Top. Catal.* 2012, *55* (7-10), 543-549.

24.Tang, J.; Zhu, L.; Fu, X.; Dai, J.; Guo, X.; Hu, C., Insights into the kinetics and reaction network of aluminum chloride-catalyzed conversion of glucose in NaCl – H_2O/thf biphasic system. *ACS Catalysis* 2017, *7* (1), 256-266.

25.Román-Leshkov, Y.; Chheda, J. N.; Dumesic, J. A., Phase modifiers promote efficient production of hydroxymethylfurfural from fructose. *Science* 2006, *312* (5782), 1933-1937.

26.Saha, B.; Abu-Omar, M. M., Advances in 5-hydroxymethylfurfural production from biomass in biphasic solvents. *Green Chem.* 2014, *16* (1), 24-38.

27.Román-Leshkov, Y.; Moliner, M.; Labinger, J. A.; Davis, M. E., Mechanism of glucose isomerization using a solid lewis acid catalyst in water. *Angew. Chem. Int. Ed.* 2010, *49* (47), 8954-8957.

28.Osatiashtiani, A.; Lee, A. F.; Granollers, M.; Brown, D. R.; Olivi, L.; Morales, G.; Melero, J. A.; Wilson, K., Hydrothermally stable, conformal, sulfated zirconia monolayer catalysts for glucose conversion to 5-hmf. *ACS Catalysis* 2015, *5* (7), 4345-4352.

29.Deng, T.; Cui, X.; Qi, Y.; Wang, Y.; Hou, X.; Zhu, Y., Conversion of carbohydrates into 5-hydroxymethylfurfural catalyzed by $ZnCl_2$ in water. *Chem. Commun.* 2012, *48* (44), 5494-5496.

30.De, S.; Dutta, S.; Saha, B., Microwave assisted conversion of carbohydrates and biopolymers to 5-hydroxymethylfurfural with aluminium chloride catalyst in water. *Green Chem.* 2011, *13* (10), 2859-2868.

31.Qi, T.; He, M.-F.; Zhu, L.-F.; Lyu, Y.-J.; Yang, H.-Q.; Hu, C.-W., Cooperative catalytic performance of lewis and brønsted acids from $AlCl_3$ salt in aqueous solution toward glucose-to-fructose isomerization. *The Journal of Physical Chemistry C* 2019, *123* (8), 4879-4891.

32.Bourcier, W. L.; Knauss, K. G.; Jackson, K. J., Aluminum hydrolysis constants to 250°C from boehmite solubility measurements. *Geochim. Cosmochim. Acta* 1993, *57* (4), 747-762.

33.Susanti; Winkelman, J. G.; Schuur, B.; Heeres, H. J.; Yue, J., Lactic acid extraction and mass transfer characteristics in slug flow capillary microreactors. *Ind. Eng. Chem. Res.* 2016, *55* (16), 4691-4702.

34.Assmann, N.; Ładosz, A.; Rudolf von Rohr, P., Continuous micro liquid-liquid extraction. *Chemical Engineering & Technology* 2013, *36* (6), 921-936.

35.Kashid, M. N.; Gerlach, I.; Goetz, S.; Franzke, J.; Acker, J. F.; Platte, F.; Agar, D. W.; Turek, S.,

Internal circulation within the liquid slugs of a liquid−liquid slug-flow capillary microreactor. *Ind. Eng. Chem. Res.* 2005, *44* (14), 5003-5010.

36.Dore, V.; Tsaoulidis, D.; Angeli, P., Mixing patterns in water plugs during water/ionic liquid segmented flow in microchannels. *Chem. Eng. Sci.* 2012, *80*, 334-341.

37.Yue, J., Multiphase flow processing in microreactors combined with heterogeneous catalysis for efficient and sustainable chemical synthesis. *Catal. Today* 2018, *308*, 3-19.

38.Kohl, T. M.; Bizet, B.; Kevan, P.; Sellwood, C.; Tsanaktsidis, J.; Hornung, C. H., Efficient synthesis of 5-(chloromethyl)furfural (CMF) from high fructose corn syrup (HFCS) using continuous flow processing. *Reaction Chemistry & Engineering* 2017, *2* (4), 541-549.

39.Muranaka, Y.; Nakagawa, H.; Masaki, R.; Maki, T.; Mae, K., Continuous 5-Hydroxymethylfurfural Production from Monosaccharides in a Microreactor. *Ind. Eng. Chem. Res.* 2017, *56* (39), 10998-11005.

40.Shimanouchi, T.; Kataoka, Y.; Yasukawa, M.; Ono, T.; Kimura, Y., Simplified model for extraction of 5-hydroxymethylfurfural from fructose: use of water/oil biphasic system under high temperature and pressure conditions. *Solvent Extraction Research and Development, Japan* 2013, *20*, 205-212.

41.Shimanouchi, T.; Kataoka, Y.; Tanifuji, T.; Kimura, Y.; Fujioka, S.; Terasaka, K., Chemical conversion and liquid–liquid extraction of 5-hydroxymethylfurfural from fructose by slug flow microreactor. *AIChE J.* 2016, *62* (6), 2135-2143.

42.Tuercke, T.; Panic, S.; Loebbecke, S., Microreactor process for the optimized synthesis of 5-hydroxymethylfurfural: a promising building block obtained by catalytic dehydration of fructose. *Chemical Engineering & Technology* 2009, *32* (11), 1815-1822.

43.Brasholz, M.; von Kanel, K.; Hornung, C. H.; Saubern, S.; Tsanaktsidis, J., Highly efficient dehydration of carbohydrates to 5-(chloromethyl)furfural (CMF), 5-(hydroxymethyl)furfural (HMF) and levulinic acid by biphasic continuous flow processing. *Green Chem.* 2011, *13* (5), 1114-1117.

44.Wang, K.; Zhang, J.; H. Shanks, B.; Brown, R. C., Catalytic conversion of carbohydrate-derived oxygenates over HZSM-5 in a tandem micro-reactor system. *Green Chem.* 2015, *17* (1), 557-564.

45.Weingarten, R.; Kim, Y. T.; Tompsett, G. A.; Fernández, A.; Han, K. S.; Hagaman, E. W.; Conner, W. C.; Dumesic, J. A.; Huber, G. W., Conversion of glucose into levulinic acid with solid metal(IV) phosphate catalysts. *J. Catal.* 2013, *304*, 123-134.

46.Moliner, M.; Román-Leshkov, Y.; Davis, M. E., Tin-containing zeolites are highly active catalysts for the isomerization of glucose in water. *Proc. Natl. Acad. Sci.* 2010, *107* (14), 6164-6168.

47.Tewari, Y. B., Thermodynamics of industrially-important, enzyme-catalyzed reactions. *Appl. Biochem. Biotechnol.* 1990, *23* (3), 187-203.

48.Fachri, B. A.; Abdilla, R. M.; Bovenkamp, H. H. v. d.; Rasrendra, C. B.; Heeres, H. J., Experimental and kinetic modeling studies on the sulfuric acid catalyzed conversion of d-fructose to 5-hydroxymethylfurfural and levulinic acid in water. *ACS Sustainable Chem. Eng.* 2015, *3* (12), 3024-3034.

49.Swift, T. D.; Bagia, C.; Choudhary, V.; Peklaris, G.; Nikolakis, V.; Vlachos, D. G., Kinetics of homogeneous Brønsted acid catalyzed fructose dehydration and 5-hydroxymethyl furfural rehydration: A combined experimental and computational study. *ACS Catalysis* 2014, *4* (1), 259-267.

50.Kallury, R. K. M. R.; Ambidge, C.; Tidwell, T. T.; Boocock, D. G. B.; Agblevor, F. A.; Stewart, D. J., Rapid hydrothermolysis of cellulose and related carbohydrates. *Carbohydr. Res.* 1986, *158*, 253-261.

51.Luijkx, G. C. A.; van Rantwijk, F.; van Bekkum, H., Hydrothermal formation of 1,2,4-benzenetriol from 5-hydroxymethyl-2-furaldehyde and d-fructose. *Carbohydr. Res.* 1993, *242*, 131-139.
52.Démolis, A.; Essayem, N.; Rataboul, F., Synthesis and applications of alkyl levulinates. *ACS Sustainable Chem. Eng.* 2014, *2* (6), 1338-1352.
53.Dunlop, A. P., Furfural Formation and Behavior. *Ind. Eng. Chem. Res.* 1948, *40* (2), 204-209.
54.Williams, D. L.; Dunlop, A. P., Kinetics of furfural destruction in acidic aqueous media. *Ind. Eng. Chem. Res.* 1948, *40* (2), 239-241.
55.Tan-Soetedjo, J. N. M.; van de Bovenkamp, H. H.; Abdilla, R. M.; Rasrendra, C. B.; van Ginkel, J.; Heeres, H. J., Experimental and kinetic modeling studies on the conversion of sucrose to levulinic acid and 5-hydroxymethylfurfural using sulfuric acid in water. *Ind. Eng. Chem. Res.* 2017, *56* (45), 13228-13239.
56.Girisuta, B.; Janssen, L.; Heeres, H., Green chemicals: A kinetic study on the conversion of glucose to levulinic acid. *Chem. Eng. Res. Des.* 2006, *84* (5), 339-349.
57.Girisuta, B.; Janssen, L. P. B. M.; Heeres, H. J., Kinetic study on the acid-catalyzed hydrolysis of cellulose to levulinic acid. *Ind. Eng. Chem. Res.* 2007, *46* (6), 1696-1708.
58.Tzoupanos, N. D.; Zouboulis, A. I.; Tsoleridis, C. A., A systematic study for the characterization of a novel coagulant (polyaluminium silicate chloride). *Colloids and Surfaces A: Physicochemical and Engineering Aspects* 2009, *342* (1), 30-39.
59.Tang, J.; Guo, X.; Zhu, L.; Hu, C., Mechanistic study of glucose-to-fructose isomerization in water catalyzed by $[Al(OH)_2(aq)]^+$. *ACS Catalysis* 2015, *5* (9), 5097-5103.
60.Atanda, L.; Shrotri, A.; Mukundan, S.; Ma, Q.; Konarova, M.; Beltramini, J., Direct production of 5-hydroxymethylfurfural via catalytic conversion of simple and complex sugars over phosphated TiO_2. *ChemSusChem* 2015, *8* (17), 2907-2916.
61.Candu, N.; El Fergani, M.; Verziu, M.; Cojocaru, B.; Jurca, B.; Apostol, N.; Teodorescu, C.; Parvulescu, V. I.; Coman, S. M., Efficient glucose dehydration to HMF onto Nb-BEA catalysts. *Catal. Today* 2019, *325*, 109-116.
62.Li, X.; Zhang, Y.; Xia, Q.; Liu, X.; Peng, K.; Yang, S.; Wang, Y., Acid-free conversion of cellulose to 5-(hydroxymethyl)furfural catalyzed by hot seawater. *Ind. Eng. Chem. Res.* 2018, *57* (10), 3545-3553.
63.Yue, J.; Boichot, R.; Luo, L.; Gonthier, Y.; Chen, G.; Yuan, Q., Flow distribution and mass transfer in a parallel microchannel contactor integrated with constructal distributors. *AIChE J.* 2010, *56* (2), 298-317.

Supplementary Material – Chapter 4

Table of contents

S4.1. Calculation of the residence time and actual phasic flow rate under the reaction temperature in the microreactor

The residence time in the microreactor (τ) was calculated according to the following equations:

$$\tau = \frac{L_C}{U_M} \tag{S4.1}$$

$$U_M = \frac{Q_{M,0}\alpha_M}{\frac{\pi}{4}D_i^2} \tag{S4.2}$$

where L_C is the length of the capillary microreactor (i.e., the section inside the heating oven) and U_M the average velocity of the two-phase mixture in the microreactor. $Q_{M,0}$ represents the total volumetric flow rate of the two-phase mixture at the microreactor inlet (i.e., at ca 20 ℃) and D_i the microreactor inner diameter. α_M denotes the ratio of the change in the total volumetric flow rate of the two-phase mixture after mixing at the reaction temperature.

The flow rates of both the aqueous and organic phases at the microreactor inlet were set by the HPLC pump unit at ca. 20 ℃. After the two phases were introduced into the microreactor to form a slug flow in the oven (Fig. 4.1), the temperature of the mixture was increased from 20 ℃ to typically 160 ℃, which caused a flow rate change of each phase due to both the miscibility change of the two phases and the density change at different temperatures. The actual total flow rate in the microreactor at the reaction temperature was thus corrected by the total volumetric flow rate change ratio (α_M). α_M was estimated using Aspen Plus simulation (version 7.3, Aspen Technology, Inc.) with an NRTL-RK thermodynamic model. The simulation dealt with a mixing process as shown in Fig. S4.1. Water and MIBK, initially at 20 ℃, were introduced into a decanter the temperature of which was kept at 160 °C. After mixing and separation in the decanter, the two phases flowed out as separate streams at 160 °C. The whole system pressure was maintained at 10 bar. The results of the volumetric flow rate change from 20 to 160 °C according to the simulation were summarized in Table S4.1. In the table, *Q* represents the volumetric flow rate and *α* the ratio of the volumetric flow rates between the decanter outlet (at 160 °C) and inlet (at 20 °C). The subscripts *aq*, *org* and *M* refer to the aqueous phase, the organic phase and the two-phase mixture, respectively. It is noticed that at an MIBK to water inlet flow rate ratio of 4:1, the outlet flow rate of MIBK phase increased significantly due to the density decrease and the dissolving of water into MIBK. As a consequence, the outlet flow rate of water phase decreased.

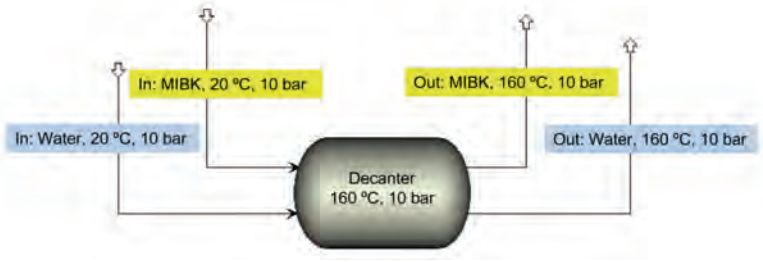

Fig. S4.1. Simulated process flow diagram for the mixing and separation of water and MIBK at 160 °C and 10 bar using Aspen Plus.

Table S4.1. Volumetric flow rate change from 20 to 160 °C according to the Aspen Plus simulation.

Inlet flow rate ratio (MIBK : water)	Q_{org} (mL/min)		α_{org} (-)	Q_{aq} (mL/min)		α_{aq} (-)	Q_M (mL/min)		α_M (-)
	Inlet (20 °C)	Outlet[a] (160 °C)		Inlet (20 °C)	Outlet[a] (160 °C)		Inlet (20 °C)	Outlet[a] (160 °C)	
4:1	400	509.05	1.273	100	89.89	0.899	500	598.94	1.198
2:1	200	253.42	1.267	100	104.76	1.048	300	358.18	1.194
1:1	100	125.61	1.256	100	112.19	1.122	200	237.80	1.189
1:2	100	123.39	1.234	200	231.82	1.159	300	355.21	1.184
1:4	100	118.97	1.190	400	471.07	1.178	500	590.04	1.180

[a] after two-phase mixing.

An example of the residence time calculation in the microreactor is provided for a known reaction condition ($Q_{M,0}$ = 0.502 mL/min, D_i = 1.65 mm, L_C = 4.5 m, an organic to aqueous inlet volumetric flow ratio at 4:1, a feed temperature of 20 °C, a reaction temperature of 160 ℃) as follows:

From Table S4.1, it is obtained that for the organic to aqueous inlet flow ratio at 4:1, $\alpha_M = 1.198$. Then, U_M was calculated according to Eq. S4.2 as

$$U_M = \frac{0.502 \times 10^{-6} \times 1.198}{60 \times \frac{\pi}{4} \times (1.65 \times 10^{-3})^2} = 4.7 \times 10^{-3} \text{ m/s} \quad \text{(S4.3)}$$

As a result, τ was derived according to Eq. S4.1 as

$$\tau = \frac{4.5}{4.72 \times 10^{-3}} = 957 \text{ s} \approx 16 \text{ min} \quad \text{(S4.4)}$$

An example list of the residence time values in the microreactor as a function of the total inlet volumetric flow rate is provided in Table S4.2.

Table S4.2. Residence time in the microreactor as a function of the total inlet volumetric flow rate.

τ^a (min)	$Q_{M,0}{}^b$ (mL/min)
2	4.019
4	2.01
6	1.34
8	1.005
12	0.67
16	0.502
20	0.402

[a] at 160 °C, based on the microreactor with a length of 4.5 m and an inner diameter of 1.65 mm. [b] at 20 °C and an organic (MIBK) to aqueous inlet volumetric flow ratio at 4:1.

S4.2. Calculation of the flow rate change ratio between the microreactor inlet and outlet

Due to the partial miscibility between MIBK and water, the aqueous or organic phase flow rate at the microreactor outlet differed from that at the inlet, although temperatures at both locations were around the same (ca. 20 °C). This flow rate change ratio was calculated using Aspen Plus in a similar way to that described in Section S1 above. A simulated mixing process was established as shown in Fig. S4.2.

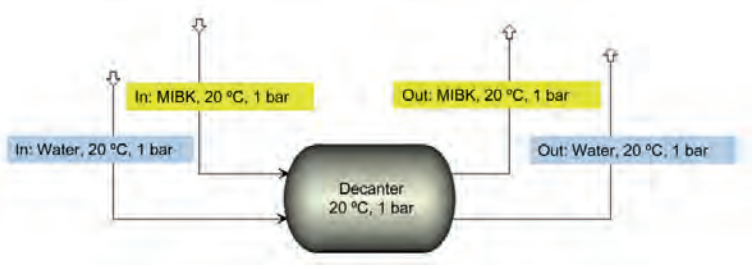

Fig. S4.2. Simulated process flow diagram for the mixing and separation of water and MIBK at 20 °C and 1 bar using Aspen Plus.

Under the conditions that the aqueous phase and MIBK phase were mixed and then separated at 20 ℃, the simulation results of the flow rate changes were summarized in Table S4.3. In the table, α represents the ratio of the volumetric flow rates between the decanter outlet and inlet (both at ca. 20 °C).

Table S4.3. Volumetric flow rate change at 20 °C after mixing according to the Aspen Plus simulation.

Inlet flow rate ratio (MIBK : water)	Q_{org} (mL/min)		α_{org} (-)	Q_{aq} (mL/min)		α_{aq} (-)
	Inlet (20 °C)	Outlet[a] (20 °C)		Inlet (20 °C)	Outlet[a] (20 °C)	
4:1	400	400.78	1.002	100	96.46	0.965
2:1	200	199.13	0.996	100	99.48	0.995
1:1	100	98.30	0.983	100	100.99	1.010
1:2	100	95.77	0.958	200	203.49	1.018
1:4	100	90.70	0.907	400	408.48	1.021

[a] after two-phase mixing and separation.

4

S4.3. Levulinic acid conversion experiments in the microreactor

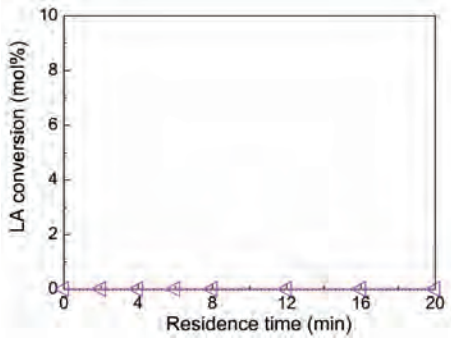

Fig. S4.3. Levulinic acid conversion in the slug flow capillary microreactor. Reaction conditions: 0.1 M LA, microreactor length of 4.5 m, 160 °C, 40 mM $AlCl_3$ and 40 mM HCl (pH = 1.5 measured at 20 ℃), 4:1 organic to aqueous volumetric flow ratio at the microreactor inlet (the organic phase refers to MIBK unless otherwise specified).

S4.4. Additional experiments on the glucose conversion to HMF with different $AlCl_3$ concentrations in the microreactor

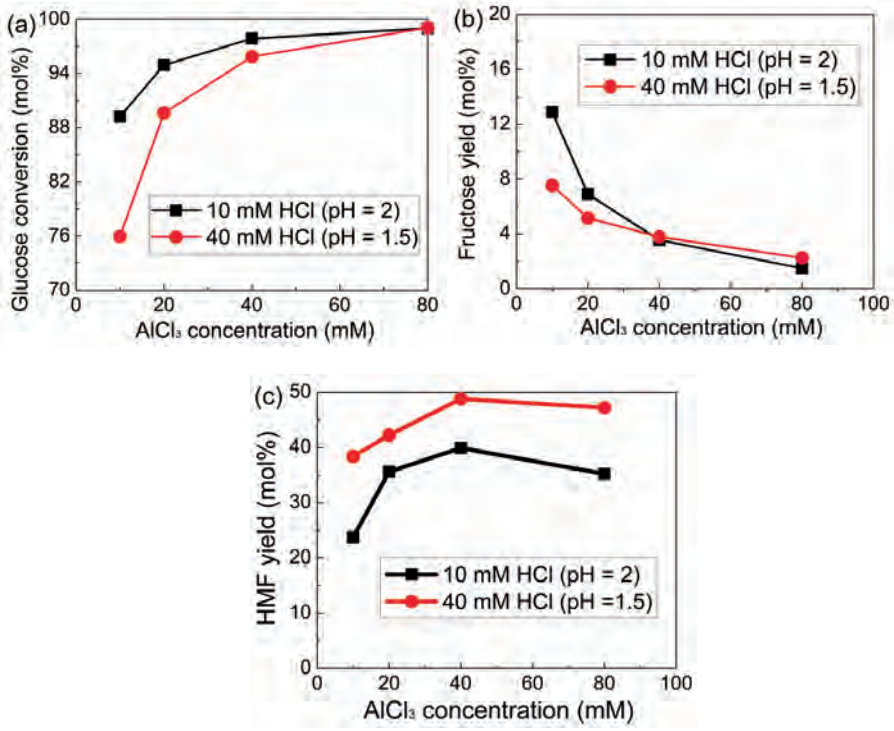

Fig. S4.4. Additional experimental results on (a) the glucose conversion, (b) the fructose yield and (c) the HMF yield using a combination of $AlCl_3$ and HCl as catalyst in the slug flow capillary microreactor. Reaction conditions: 0.1 M glucose, 160 °C, microreactor length of 4.5 m, residence time at 16 min, pH was adjusted by the addition of HCl and measured at ca. 20 °C, 4:1 organic to aqueous inlet flow ratio.

S4.5. Effect of Brønsted acidity on the glucose conversion using HCl as catalyst in the microreactor

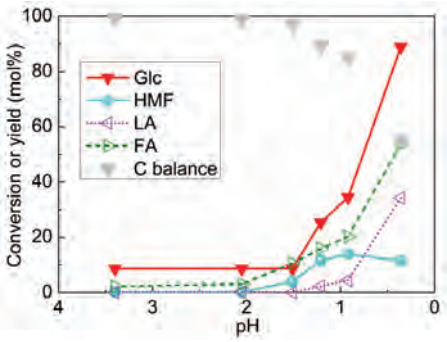

Fig. S4.5. Effect of Brønsted acidity on the glucose conversion reaction performance using HCl as catalyst in the slug flow capillary microreactor. Reaction conditions: 0.1 M glucose, 160 °C, microreactor length of 4.5 m, residence time at 16 min, pH was adjusted by the addition of HCl and measured at ca. 20 °C, 4:1 organic to aqueous inlet flow ratio.

S4.6. Glucose conversion with different glucose concentrations and catalyst loadings

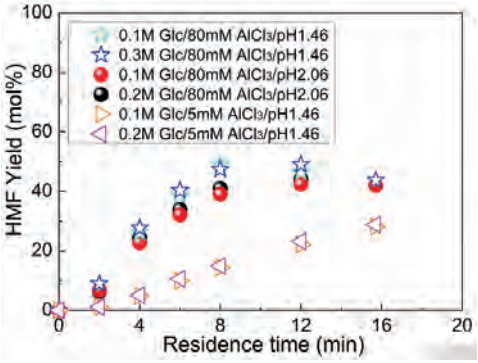

Fig. S4.6. HMF yield in the reaction starting with different concentrations of glucose and $AlCl_3$ catalyst in the slug flow capillary microreactor. Other reaction conditions: 160 °C, microreactor length of 4.5 m, residence time at ca. 16 min, 4:1 MIBK to aqueous inlet flow ratio, pH values were adjusted by the addition of HCl in the aqueous phase and reported according to measurement at ca. 20 °C.

S4.7. Experiments in a laboratory batch reactor

Experiments on the glucose conversion to HMF over the combined $AlCl_3$/HCl catalyst were performed in a laboratory batch reactor in a water-MIBK biphasic system. Ace pressure tubes (height of 10.2 cm; outer diameter of 19 mm) were used as the batch reactor and were

supplied by Sigma-Aldrich Co., Ltd. In a typical run, 1 mL of the aqueous reactant solution and 4 mL of MIBK were added into the pressure tubes, followed by being sealed and heated at 160 ^{o}C for a certain duration under magnetic stirring at 500 rpm in an oil bath. At the end of the reaction, the tubes were quenched in cooled water (at ca. 20 ^{o}C), and then the aqueous phase and the organic phase were filtered before their analysis by HPLC and GC, respectively.

The conversion of substrate i (X_i) and yield of product j (Y_j) in the batch reactor are defined by Eqs. S4.5 and S4.6.

$$X_i = \frac{V_{aq,0}C_{aq,i,0} - V_{aq,1}C_{aq,i,1}}{V_{aq,0}C_{aq,i,0}} \times 100\% \quad \text{(S4.5)}$$

$$Y_j = \frac{V_{org,1}C_{org,j,1} + V_{aq,1}C_{aq,j,1}}{V_{aq,0}C_{aq,i,0}} \times 100\% \quad \text{(S4.6)}$$

In the above equations, $V_{aq,0}$ and $V_{org,0}$ designate the volumes of the aqueous and organic phases at the start of the reaction (i.e., at ca 20 ^{o}C), respectively. $V_{aq,1}$ and $V_{org,1}$ are the volume of the aqueous and organic phases at the end of the reaction (i.e., after being cooled to ca. 20 ^{o}C), respectively. $C_{aq,i,0}$ and $C_{aq,i,1}$ refer to the concentrations of substrate i in the aqueous solutions at the start and end of the reaction, respectively. $C_{aq,j,1}$ and $C_{org,j,1}$ represent the concentrations of product j in the aqueous and organic phases at the end of the reaction, respectively. Due to the partial miscibility of MIBK and water, $V_{aq,1}$ and $V_{org,1}$ differ from $V_{aq,0}$ and $V_{org,0}$, and were corrected as

$$V_{aq,1} = V_{aq,0}\alpha_{aq} \quad \text{(S4.7)}$$

$$V_{org,1} = V_{org,0}\alpha_{org} \quad \text{(S4.8)}$$

where α_{aq} or α_{org} is the correction factor which represents the ratio of the volume at the end and start of the reaction for either the aqueous or organic phase. The values of α_{aq} and α_{org} are found in Table S4.3 for a given initial MIBK to water volume ratio (equal to the inlet MIBK to water flow rate ratio shown in the table).

Fig. S4.7 shows the optimized results of HMF synthesis from glucose in a biphasic system in the batch reactor. The reaction rates (in terms of the glucose conversion and HMF yield) appeared to be much higher in the slug flow capillary microreactor than in batch (via a comparison between Figs. 2 and S7). Yields of other byproducts (such as FA and LA) are also

higher in the microreactor at the same reaction time, and intermediates (such as fructose and mannose) were formed and consumed earlier in the microreactor as well.

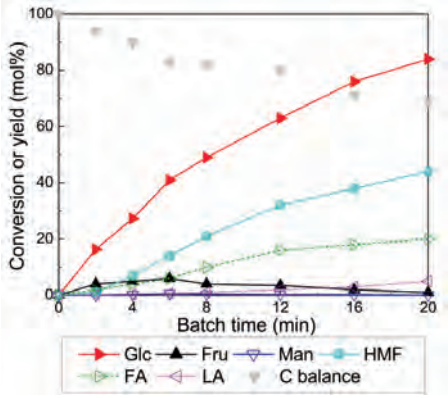

Fig. S4.7. Optimized results of HMF synthesis from glucose in a biphasic system in the batch reactor. Reaction conditions: 0.1 M glucose, 160 °C, 500 rpm, 40 mM $AlCl_3$ and 40 mM HCl (pH = 1.5 measured at ca. 20 °C), 4:1 organic to aqueous initial volume ratio.

To check whether there was a mass transfer limitation in the batch reactor, the effect of stirring speed on the glucose conversion reaction was studied. As shown in Fig. S4.8, the glucose conversion and HMF yield were almost unchanged at a stirring speed of 400 rpm or above. Thus, the current batch results (at 500 rpm) were obtained without the presence of a mass transfer limitation.

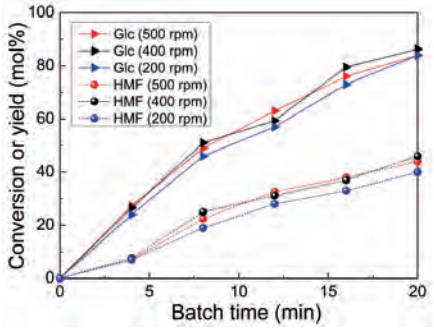

Fig. S4.8. Glucose conversion and HMF yield in the batch reactor at different stirring speeds. Reaction conditions: 0.1 M glucose, 160 °C, 40 mM $AlCl_3$ and 40 mM HCl (pH = 1.5 measured at ca. 20 °C), 4:1 organic to aqueous volume ratio.

S4.8. Measurement and calculation of the heating profile of different liquids in the batch reactor and microreactor

Fig. S4.9 presents the temperature measured in the batch reactor (in the presence of an aqueous glucose solution and MIBK at an organic to aqueous volume ratio of 4:1) and that estimated in the microreactor (with a laminar flow of water or MIBK) at different reaction time values, both reactors being heated to a target reaction temperature of 160 °C.

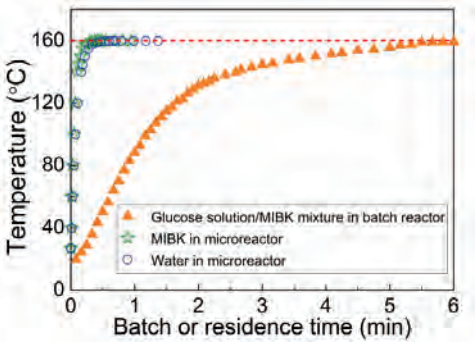

Fig. S4.9. Heating profile of different liquids in the batch reactor and microreactor with the set temperature at 160 °C. The batch reactor data were obtained using the same pressure tubes (cf. Section S7) at 500 rpm with a thermocouple inserted to measure the temperature of the mixture containing 0.1 M glucose solution (with 40 mM $AlCl_3$ and 40 mM HCl) and MIBK. The microreactor data were calculated according to the simplified case of water or MIBK laminar flow therein. A constant temperature line at 160 °C is shown for visual guidance.

The method for calculating the temperature of MIBK or water flowing in the capillary microreactor at different residence times is shown hereafter. According to the heat transfer process as schematically shown in Fig. S4.10, it is easy to obtain that over a differential length (*dL*) of the microreactor, there is

$$d\phi_H = h_1 \pi D_e (T_{air} - T_{air,W}) dL = \frac{2\pi\lambda_C (T_{air,W} - T_{feed,W}) dL}{\ln\left(\frac{D_e}{D_i}\right)} = h_2 \pi D_i (T_{feed,W} - T_{feed}) dL \quad \text{(S4.9)}$$

Here ϕ_H represents the heat transfer rate between air in the oven and the feed in the microreactor. T_{air}, $T_{air,W}$, $T_{feed,W}$ and T_{feed} denote the air temperature values inside the oven and on the microreactor outer wall, the feed temperature on the microreactor inner wall and the average temperature of the feed inside the microreactor, respectively. h_1 and h_2 are the heat

transfer coefficients from air in the oven to the microreactor outer wall, and from the microreactor inner wall to the feed, respectively. λ_C is the thermal conductivity of the microreactor. D_e and D_i are the outer and inner diameters of the microreactor, respectively.

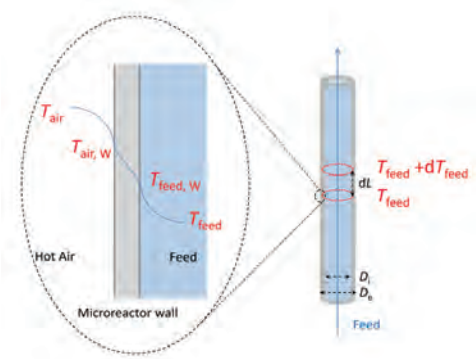

Fig. S4.10. Scheme of heating transfer process under single-phase laminar flow in the capillary microreactor.

Eq. S4.9 can be rearranged as

$$d\phi_H = U(T_{air} - T_{feed})\pi D_e dL \tag{S4.10}$$

where U represents the total heat transfer coefficient defined as

$$U = \frac{1}{\frac{1}{h_1} + \frac{D_e \ln\left(\frac{D_e}{D_i}\right)}{2\lambda_C} + \frac{D_e}{h_2 D_i}} \tag{S4.11}$$

A heat balance analysis of the feed over a differential volume of the microreactor (cf. Fig. S4.10) leads to

$$Q\rho C_P dT_{feed} = U(T_{air} - T_{feed})\pi D_e dL \tag{S4.12}$$

where Q, ρ and C_P represent the volumetric flow rate, density and specific heat of the feed, respectively.

A rearrangement and integration of Eq. S4.12 over a certain microreactor length from the inlet yields

$$\int_{T_{feed,0}}^{T_{feed,1}} \frac{Q\rho C_P}{T_{air} - T_{feed}} dT_{feed} = \int_0^L U\pi D_e dL \tag{S4.13}$$

where the subscripts 0 and 1 represent the microreactor inlet and a downstream position at

a length of *L*, respectively. Thus, it is finally obtained that

$$L = \frac{Q\rho C_p}{U\pi D_e} \ln\left(\frac{T_{air} - T_{feed,0}}{T_{air} - T_{feed,1}}\right) \quad \text{(S4.14)}$$

In the above equation, a constant total heat transfer coefficient throughout the system and a constant fluid property (e.g., ρ and *Cp*; which can be taken as the value at the average temperature of the feed between the microreactor inlet and a certain downstream position) were assumed. For the microreactor section in which the fluid was heated from 20 ℃ to 160 ℃, the average temperature of the feed ($T_{feed,m}$) is:

$$T_{feed,m} = \frac{T_{feed,0} + T_{feed,1}}{2} = \frac{20 + 160}{2} = 90\ ^\circ\text{C} \quad \text{(S4.15)}$$

At this temperature, the physiochemical properties of water and MIBK are shown in Table S4.4.

Table S4.4. Properties of water and MIBK at 90 °C[1].

Feed	C_p (J/(g·K))	ρ (g/mL)	λ_f[a] (W/(m·K))	μ[b] (mPa·s)
Water	4.195	0.969	0.672	0.335
MIBK	2.281	0.740	0.127	0.293

[a] Thermal conductivity of the feed; [b] Viscosity of the feed.

The temperature inside the oven was measured at different positions (including that on the microreactor outside wall), and it turned out that the temperature was quite uniform. Thus, the external heat transfer resistance from the oven to the microreactor outer wall was neglected to simplify the heat transfer process, namely,

$$\frac{1}{h_1} \approx 0 \quad \text{(S4.16)}$$

The fluid flow pattern inside the microreactor was determined by Reynolds number (*Re*):

$$\text{Re} = \frac{D_i \rho u}{\mu} \quad \text{(S4.17)}$$

where *u* is the average velocity of the feed in the microreactor and calculated as

$$u = \frac{Q}{\frac{\pi}{4} D_i^2} \quad \text{(S4.18)}$$

For laminar flow conditions prevalent in the microreactor (*Re* < 2200), the heat transfer

process inside the microreactor can be approximately described by

$$Nu = \frac{h_2 D_i}{\lambda_f} = 3.66 \tag{S4.19}$$

Here *Nu* is the Nusselt number. Strictly speaking, the above correlation is valid with constant wall temperature condition under a thermally fully developed laminar flow[2]. In the current case, only the microreactor outer wall temperature was constant (i.e., $T_{air,W} = T_{air} = 160$ °C) and the inner wall temperature might change depending on the heat transfer rate difference along the microreactor. However, for a first approximation the actual value of *Nu* is expected to be on a similar level, which is sufficient for a qualitative analysis here.

Based on the above analysis, *U* can be approximated as

$$U = \frac{1}{\frac{D_e \ln\left(\frac{D_e}{D_i}\right)}{2\lambda_C} + \frac{D_e}{3.66\lambda_f}} \tag{S4.20}$$

By combining Eqs. S4.14 and S4.20, we can estimate the residence time needed to reach a certain temperature level or the target reaction temperature (i.e., at 160 °C in this case) as

$$\tau = \frac{L}{u} = \frac{\rho C_p D_i^2}{4UD_e} \ln\left(\frac{T_{air} - T_{feed,0}}{T_{air} - T_{feed,1}}\right) \tag{S4.21}$$

An example is given below for the estimation of the heating profile in the microreactor.

The temperature of air in the oven (T_{air}) is 160 °C, the initial temperature of feed ($T_{feed,0}$) is 20 °C, the inner diameter of microreactor (D_i) is 1.65 mm and the external diameter (D_e) 3.18 mm, the thermal conductivity of PFA microreactor material (λ_C) is 0.209 W/(m·K). Then, the total heat transfer coefficient in the case of laminar flow of water is estimated according to Eq. S4.20 as

$$U = \frac{1}{\frac{3.18\times10^{-3}\times\ln\left(\frac{3.18}{1.65}\right)}{2\times0.209} + \frac{3.18\times10^{-3}}{3.66\times0.672}} = 159.11 \ \text{W/(m}^2\text{K)} \tag{S4.22}$$

The residence time needed to heat water in the microreactor to a certain temperature ($T_{feed,1}$) is further estimated according to Eq. S4.21 as

$$\tau = \frac{0.969\times10^3\times4.195\times10^3\times(1.65\times10^{-3})^2}{4\times159.11\times3.18\times10^{-3}} \ln\left(\frac{160-20}{160-T_{feed,1}}\right) = 5.468\ln\left(\frac{140}{160-T_{feed,1}}\right) \ \text{s} \tag{S4.23}$$

Then, the heating profile of the feed (i.e., water temperature as a function of the residence time) is obtained as

$$T_{feed,1} = 160 - 140e^{-\frac{\tau}{5.468}} \quad \text{(S4.24)}$$

The heating profile in the case of a laminar flow of MIBK can be estimated similarly as

$$T_{feed,1} = 160 - 140e^{-\frac{\tau}{4.266}} \quad \text{(S4.25)}$$

It has to be noted that the above calculations in the microreactor are based on the simplified single-phase laminar flow (of water or MIBK). In the case of a water-MIBK biphasic system in the microreactor, the two-phase heat transfer is further enhanced due to the internal circulation present in both droplets and slugs[3]. Therefore, the heating time could be further shortened compared with the single-phase flow case (e.g., smaller than 20 s with reference to Fig. S4.9).

S4.9. Definition and calculation of the space time yield in the batch reactor and microreactor

The space time yields of HMF in the batch and microreactor are defined in Eqs. S4.26 and S4.27, respectively.

$$\text{Space time yield in batch} = \frac{V_{aq,1}C_{aq,HMF,1} + V_{org,1}C_{org,HMF,1}}{t(V_{aq,1} + V_{org,1})} \quad \text{(S4.26)}$$

$$\text{Space time yield in microreactor} = \frac{Q_{org,1}C_{org,HMF,1} + Q_{aq,1}C_{aq,HMF,1}}{\frac{1}{4}\pi D_i^2 L_C} \quad \text{(S4.27)}$$

where *t* is the batch time. Examples for calculating the space time yield are shown below.

In the batch reactor tested in this work, the initial volumes of the organic phase and aqueous phase were 4 mL and 1 mL, respectively. At a batch time of 16 min, HMF concentrations in the organic phase and aqueous phase are 0.0066 and 0.006 mol/L, respectively, according to the HPLC/GC analysis. The values of volume correction factors (α_{aq} and α_{org}) are found from Table S4.3 as 0.965 and 1.002 at 4:1 MIBK-water flow/volume ratio, respectively. Then, according to Eq. S4.26 there is

$$\begin{aligned}\text{Space time yield in batch} &= \frac{V_{aq,1}C_{aq,HMF,1} + V_{org,1}C_{org,HMF,1}}{t(V_{aq,1} + V_{org,1})} \\ &= \frac{V_{aq,0}\alpha_{aq}C_{aq,HMF,1} + V_{org,0}\alpha_{org}C_{org,HMF,1}}{t(V_{aq,0}\alpha_{aq} + V_{org,0}\alpha_{org})} \\ &= \frac{1\times 0.965\times 0.006 + 4\times 1.002\times 0.0066}{16\times(1\times 0.965 + 4\times 1.002)\times 10^{-6}} \\ &= 405.22\ \text{mmol HMF}\cdot\text{min}^{-1}\cdot\text{m}^{-3}\end{aligned} \quad \text{(S4.28)}$$

In the microreactor, the inner diameter (D_i) is 1.65 mm and the length (L_C) 4.5 m. At a residence time of 16 min, the original organic flow rate ($Q_{org,0}$) is 0.402 mL/min and the aqueous flow rate ($Q_{aq,0}$) 0.1 mL/min. The corresponding HMF concentration is 0.0101 mol/L in the organic phase and 0.0087 mol/L in the aqueous phase. Then, according to Eq. S4.27 there is

$$\begin{aligned}\text{Space time yield in microreactor} &= \frac{Q_{org,1}C_{org,HMF,1} + Q_{aq,1}C_{aq,HMF,1}}{\frac{1}{4}\pi D_i^2 L_C} \\ &= \frac{Q_{org,0}\alpha_{org}C_{org,HMF,1} + Q_{aq,0}\alpha_{aq}C_{aq,HMF,1}}{\frac{1}{4}\pi D_i^2 L_c} \\ &= \frac{0.402\times 1.002\times 0.0101 + 0.1\times 0.965\times 0.0087}{0.25\times 3.14\times 0.00165^2\times 4.5} \\ &= 510.32\ \text{mmol HMF}\cdot\text{min}^{-1}\cdot\text{m}^{-3}\end{aligned} \quad \text{(S4.29)}$$

Space time yields of HMF in the batch reactor and microreactor of this work at different batch or residence times are summarized in Table S4.5. The corresponding values from some other researches were also calculated similarly, and are summarized in Table 4.2 for comparison.

Table S4.5. Space time yields of HMF in the batch reactor and microreactor of this work.[a]

Batch time or residence time (min)	Space time yield (mmol HMF · min^{-1} · m^{-3})	
	Batch reactor	Microreactor
2	188.33	351.35
4	194.16	955.14
6	313.21	1009.63
8	317.83	893.14
12	380.78	726.70
16	405.22	510.32
20	437.78	443.84

[a] 0.1 M glucose, 160 °C, 40 mM $AlCl_3$ and 40 mM HCl (pH = 1.5 measured at ca. 20 °C), organic to aqueous inlet flow ratio or initial volume ratio at 4 : 1.

References

1. NIST Chemistry WebBook, https://webbook.nist.gov/chemistry/.

2. Bird, R., B., WE Stewart and EN Lightfoot,“. Transport Phenomena”, second edition, John Wiley & Sons, Inc 2002.

3. Bandara, T.; Nguyen, N.-T.; Rosengarten, G., Slug flow heat transfer without phase change in microchannels: A review. Chem. Eng. Sci. 2015, 126, 283-295.